CRREL REPORT 90-2

AD-A228 560

# Laboratory Test for Measurement of Adhesion Strength of Spray Ice to Coated Flat Plates

Nathan D. Mulherin, Jacqueline A. Richter-Menge, Thomas J. Tantillo, Larry D. Gould, Glenn D. Durell, and Bruce C. Elder

May 1990

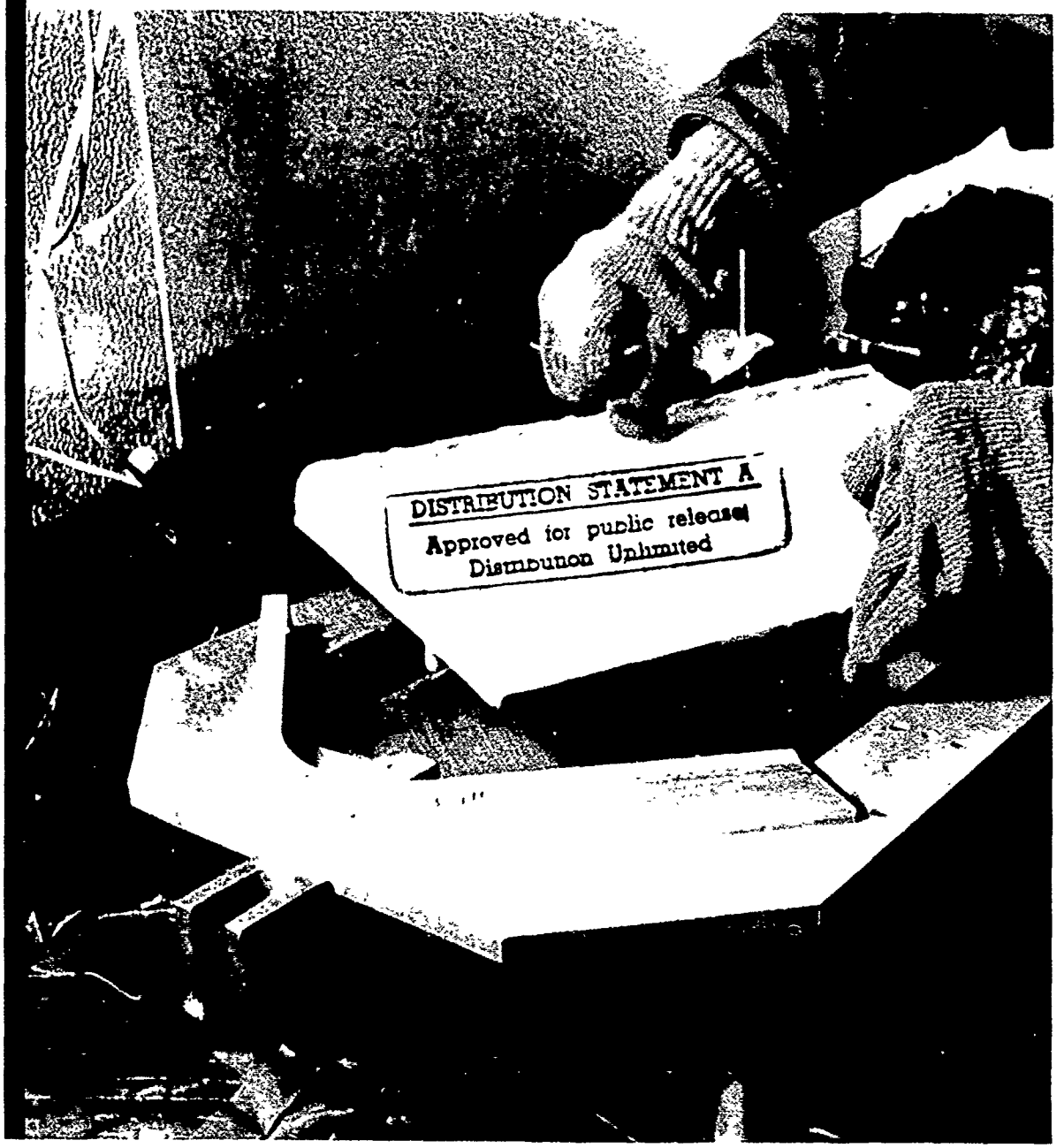

*For conversion of SI metric units to U.S./British customary units of measurement consult ASTM Standard E380,* Metric Practice Guide, *published by the American Society for Testing and Materials, 1916 Race St., Philadelphia, Pa. 19103.*

*COVER: Sample being loaded into shear fixture.*
*(Photo by R. Demars)*

CRREL Report 90-2

**U.S. Army Corps of Engineers**
Cold Regions Research & Engineering Laboratory

# Laboratory Test for Measurement of Adhesion Strength of Spray Ice to Coated Flat Plates

Nathan D. Mulherin, Jacqueline A. Richter-Menge, Thomas J. Tantillo, Larry D. Gould, Glenn D. Durell, and Bruce C. Elder

May 1990


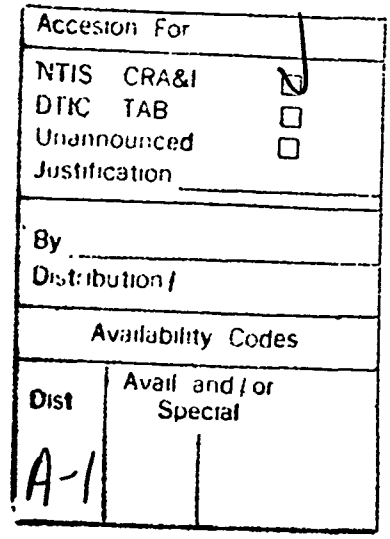


Prepared for
U.S. DEPARTMENT OF THE NAVY

## PREFACE

This report was prepared by Nathan D. Mulherin, Research Physical Scientist, Jacqueline A. Richter-Menge, Research Civil Engineer, Thomas J. Tantillo, Mechanical Engineer, Larry D. Gould, Mechanical Engineering Technician, Glenn D. Durell, Engineering Technician, and Bruce C. Elder, Student-Trainee, of the U.S. Army Cold Regions Research and Engineering Laboratory. Funding for this research was provided by the U.S. Naval Sea Systems Command under project MIPR N0002489MP, and by DA Project 4A762730AT42, *Design, Construction and Operations Technology for Cold Regions*, Task SS, *Properties of Cold Regions Materials*, Work Unit 005, *Mechanical Design for Icing Environments*.

The authors are indebted to the following people for the successful completion of this work: Dr. C.C. Ryerson for aid in the statistical analysis and technical review of the manuscript; W. Burch, R. Forrest, R. Farr, J. Stanley and R. Gallant for construction of test equipment; N. Perron for technical assistance in sample preparation and ice characterization; G. Lemieux for temperature calibration and data logger programming; T. Vaughan, E. Perkins, and W. Bates for figure preparation; E. Wright for editorial review and J. Severance for page composition.

## CONTENTS



## ILLUSTRATIONS

Figure

## ILLUSTRATIONS (cont.)



## TABLES

# Laboratory Test For Measurement of Adhesion Strength of Spray Ice To Coated Flat Plates

NATHAN D. MULHERIN, JACQUELINE A. RICHTER-MENGE, THOMAS J. TANTILLO, LARRY D. GOULD, GLENN D. DURELL, AND BRUCE C. ELDER

## INTRODUCTION

Icing by sea spray and atmospheric precipitation is a recognized problem for commercial shipping and fishing vessels. At the very worst, heavy icing can cause vessels to capsize due to loss of sea-keeping ability. Icing is also a problem in terms of preparedness for U.S. Navy vessels operating in northern latitudes. Topside components such as hatches, gun turrets, lifeboats, and firefighting and communication equipment may be rendered inoperable for long periods of time. Crewmen negotiating ice-covered decks and stairways during high sea states that accompany icing events are at grave risk. These and other difficulties have prompted a Navy effort to seek ways of mitigating the effects of topside icing (U.S. Navy 1988). The ability of surface coatings to reduce the adhesion strength of ice on superstructure and topside components and thereby make its removal easier is being investigated as a possible protection technique.

Four commercially available coatings were identified from earlier studies (Free and Chaney 1986, Zahn 1987) as strong candidates for preventing and/or easing the removal of sea spray and atmospheric icing on shipboard superstructures. The objective of this study, funded by the David Taylor Naval Ship Research and Development Center (DTRC), was to discriminate more fully between these specific candidate coatings. Our method of discrimination was to measure and compare the force required to shear a buildup of freshwater ice from flat plate test surfaces. The test used consisted of an edge load applied to the ice layer on a substrate sample. While convenient for this particular program, it may be desirable in future tests to use a distributed load application over the entire bulk of the ice to approach more closely a true shear test. The results of this laboratory study follow.

## EQUIPMENT AND PROCEDURE

### Test coatings

Twelve samples each of the four different coatings and two different control surfaces (a total of 72 samples) were subjected to distilled water spray icing and then shear tested. One control surface was the U.S. Navy's standard primer and topcoat, TTE-490, that is routinely used to paint ship superstructure. This paint system consists of a polyamide epoxy anti-corrosive base coat with a silicone alkyd enamel top coat. The candidate coatings were applied by DTRC to 0.476 cm-thick, cold-rolled steel plates that had already been painted with TTE-490. These 60 samples were individually wrapped and numbered and then shipped to CRREL for testing. The four test coatings were a fluoropolymer paint made by Fluorocarbon Technologies, Inc., and three versions of a hydrophobic silica paint produced by M-CHEM Corporation. M-CHEM's standard version of Vellox-140 and two pigmented versions, Gray Vellox and Black Vellox, were tested.

The second control group consisted of a bare, 1.27-cm-thick, cast aluminum plate. The surface finish was machined to a roughness ($R_a$) of 0.64 mm and a flatness of 0.4 mm/m by the manufacturer and was cut into test plates at CRREL. Aluminum was selected so that the plates could be reused without corrosion problems. Since the elastic modulus of aluminum is lower than that of steel, thicker plate was necessary to attain a stiffness similar to that of the steel plates. They were then washed in warm, soapy water and rinsed with acetone and distilled water. Between the two tests, the aluminum samples were again washed and rinsed as before.

All test plates measured 22.9-cm wide × 38.1-cm long. The following designations are used throughout this report in referring to the surface types:

- TTE — TE-490 (control 1)
- AL — Aluminum (control 2)
- FPC — Fluorocarbon Technologies' fluoropolymer paint
- SV — M-CHEM Corporation's standard Vellox-140
- GV — Gray Vellox
- BV — Black Vellox.

Technical data for the control and test surfaces can be obtained from the manufacturers listed in Appendix A.

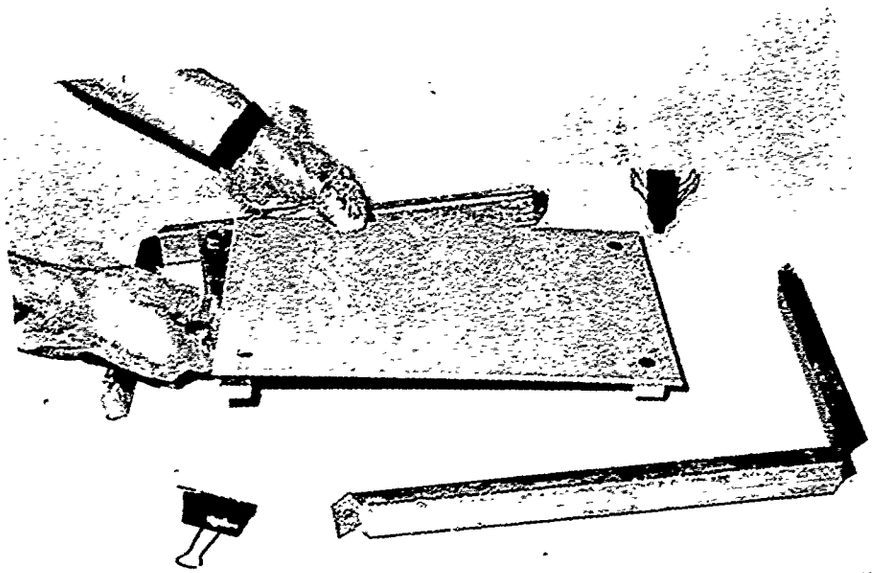

*Figure 1. Flat aluminum bars with threaded studs being attached to the test plates to allow them to be held in the shear fixture.*

Test groups were prepared consisting of one plate from each of the six surface types. The test groups are labeled according to the date that they were sprayed and prepared for shearing. For example, the samples of test group 612 were all spray iced at the same time on 12 June 89. Shear testing was always performed the day following ice buildup, which allowed the ice a minimum of 12 hours to relieve stresses that may have been introduced during the preparation procedure. All, with the exception of the aluminum plates, were shear tested only once. Since only six of the aluminum control plates were fabricated, each of these was tested twice.

**Sample preparation for spraying**

Flat aluminum mounting bars were attached at each end of a sample plate using taper-headed bolts with expansion collets in existing holes at the corners of the plate. Threaded studs in the bottom of these bars allowed the plate to be secured to the shear fixture (Fig. 1

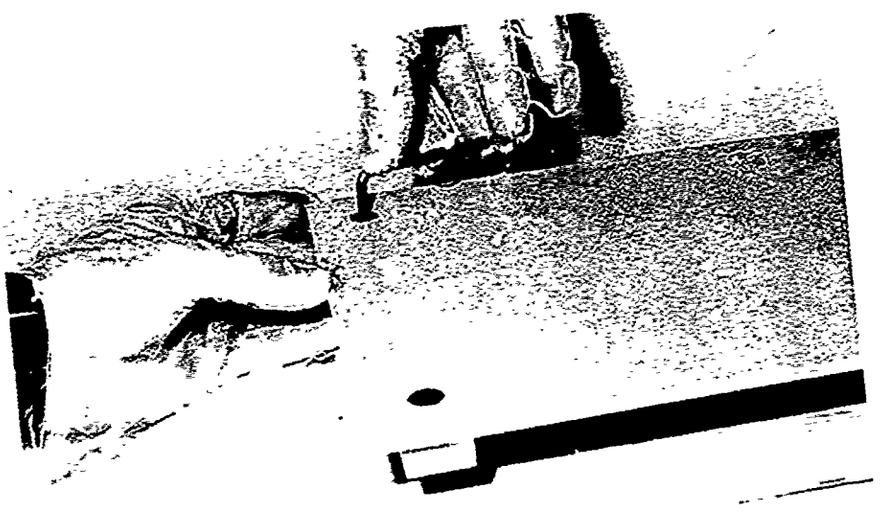

*Figure 2. Mounting bars being secured with taper-headed bolts and expansion collets.*

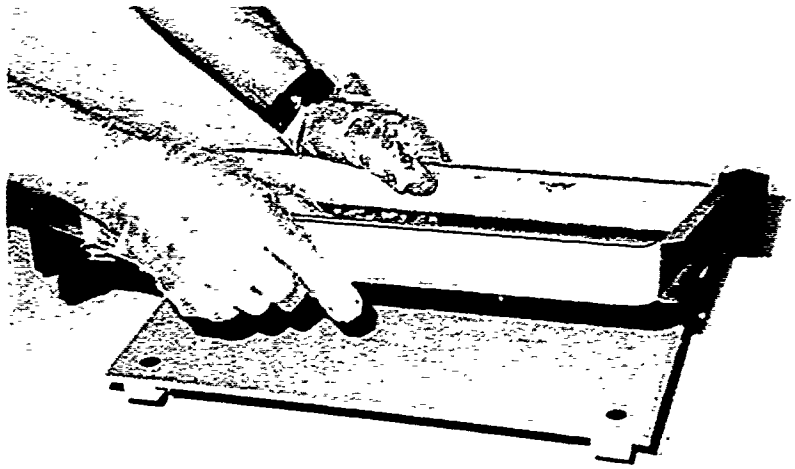

*Figure 3. Halves of a galvanized steel mold being clipped together at the corners and fitted over the sample to allow a uniform block of ice to be formed on the test plate.*

and 2). Polyethylene disposable gloves were used during the mounting operation to prevent cross contamination of samples. After the samples of a test group were fitted with mounting bars, they were taken for overnight storage to the coldroom where they would be spray iced. Extreme care was observed hereafter in keeping the test group in an air temperature of $-10 \pm 1$°C, which was the temperature we chose for performing the shear tests. The samples were stored with the surfaces covered to prevent contamination and frosting. The following morning, the samples were positioned and leveled in the spray chamber and a galvanized steel mold was clipped into place around each sample (Fig. 3). The mold acted as a dam to grow ice of uniform thickness and increase the rate of ice buildup by preventing runoff. It also reduced irregularities around the edges, and made the samples easier to handle and less subject to damage.

## Spray icing facility

The spray chamber constructed for the program was originally intended to simulate seaspray icing. However, shortage of time prevented us from perfecting a technique for growing realistic saline ice. Instead, distilled water was used for spray icing the samples. The spray chamber (Fig. 4) was a box with two overhead spray nozzles, mounting racks for horizontal placement of samples, a reservoir to charge the sprayers, and a waste tank to collect overspray. The nozzles (1/4S14WSQ) were of the BEX SW-SQ series that delivered a wide-angle, square spray pattern. The water delivery rate at our operating pressure of 70 kPa was 5.3 L/m. The air liquid water content and droplet size were not measured.

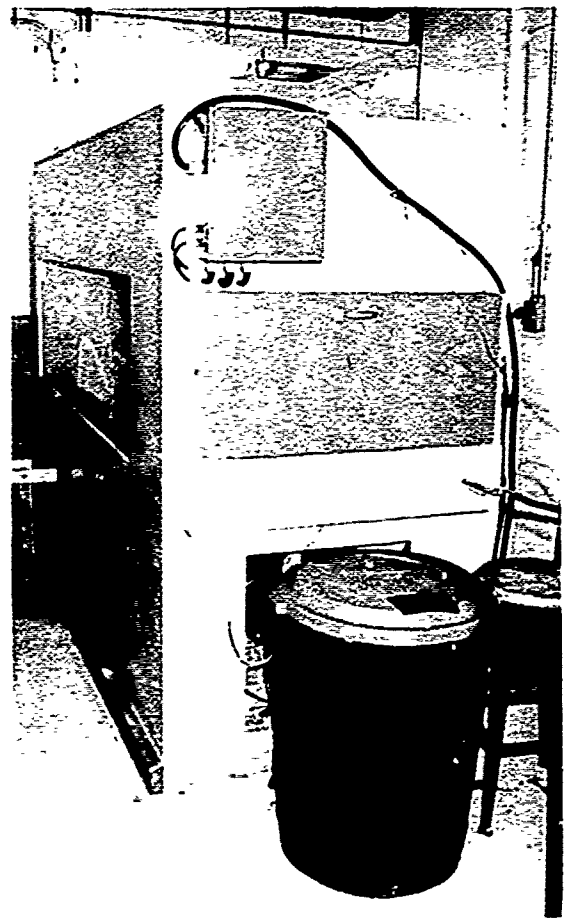

*Figure 4. Spray chamber showing the water reservoir (plastic barrel) and the control box enclosing the timed mode relay switches.*

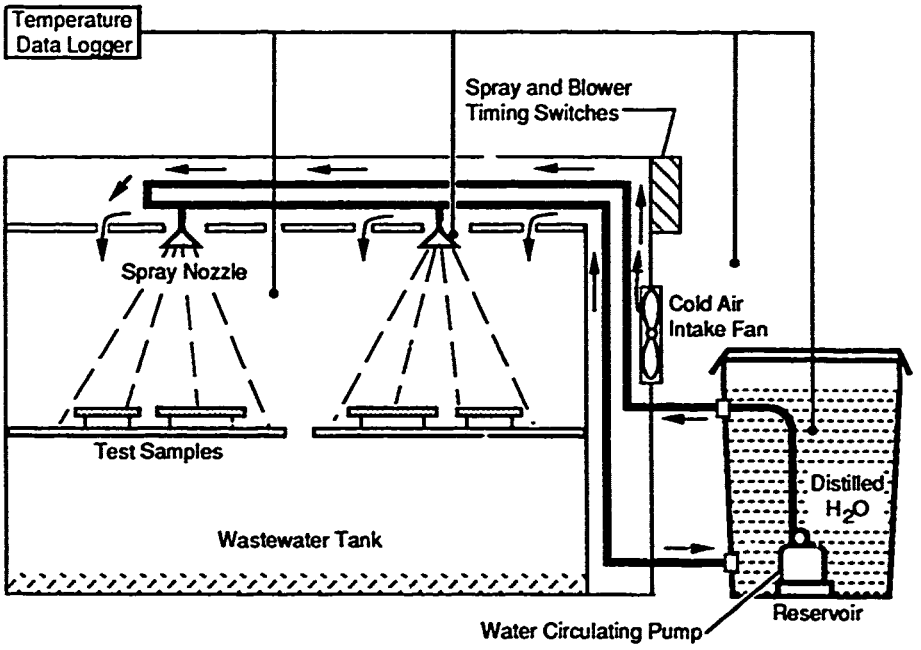


*Figure 5. Schematic diagram of the spray chamber showing the location of the temperature sensors.*

The chamber was cooled externally by its placement in a coldroom that was maintained at –12.5±2°C. A high-capacity blower circulated coldroom air throughout the chamber whenever the sprayers were off. Heat generated by the pump, blower, and the spray water kept the temperature inside the chamber at –10.0 ± 1°C. T-type thermocouples were used to monitor temperatures in the coldroom, the spray chamber, the water reservoir, and the spray nozzles (Fig. 5). The thermocouples were each read at five-minute intervals and recorded on both paper and magnetic tape using a Hewlett-Packard 3421A data acquisition system. Resolution of the thermocouples was ± 0.05°C/°C.

Relay switches with individual timers automatically and continuously cycled through three modes of operation during an icing period. During the first mode, a blower moved room air through the chamber to cool the samples. This was followed by a pause mode during which the blower shut off and the air turbulence was allowed to subside. The sprayers were activated during the third mode. The length of time for the blow and pause modes was selectable between 1 and 1022 seconds, while the spray mode was selectable between 0.1 and 102.2 seconds. Prior to actual sample icing, experimentation with sample position and length of time for the various modes was done to ensure maximum uniformity of ice growth within and between test groups.

The spray chamber was large enough to uniformly spray only six samples at one time (Fig. 6). To eliminate position as a variable in the shear tests, each surface type was rotated into each of the six available positions twice during 12 icing periods. Manual ice thickness measurements were taken at the center of each sample at least hourly during the growth periods. Resolution of the thickness measurements is ± 0.16 cm.

**Sample preparation for shearing**

When the ice had achieved at least 2.2 cm in thickness for all samples in the test group, the spray and pause modes were turned off. The blower remained on, cooling the samples for 30 minutes before they were removed from the chamber and transported in an insulated box to another coldroom for shear test preparation. The samples were allowed to cool for another hour before the steel molds were removed by heating them briefly with a handheld propane torch (Fig. 7). The rough edge around the top of the ice was then trimmed with a 60°-bevel cut using a radial arm saw with a 25.4-cm-diameter, 60-tooth, carbide-tipped blade (Fig. 8 and 9). The ice thickness at the loading edge of all the samples was recorded prior to storing them overnight at the test temperature in the insulated box in the coldroom (Fig. 10 and 11). The following day, the test group was transported to CRREL's Materials Testing Laboratory to await shear testing.

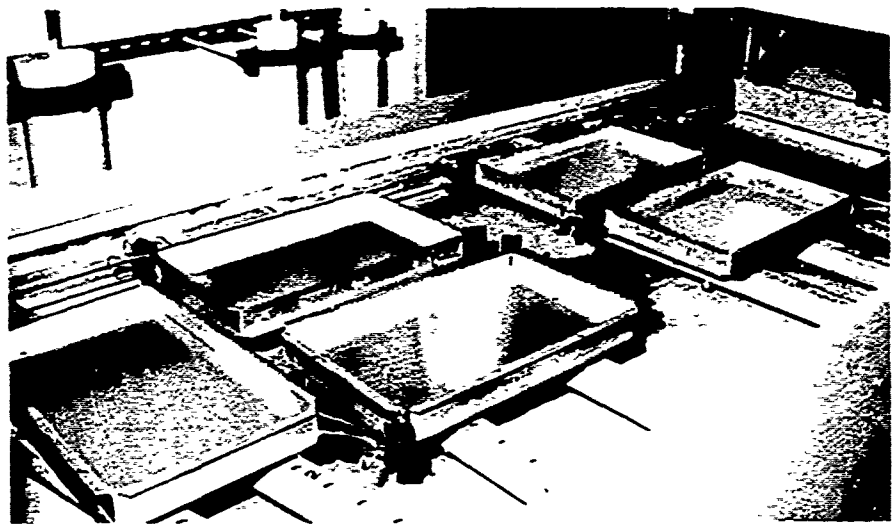

*Figure 6. Samples in spray chamber. One sample from each of the surface types made up a test group that was subjected to spray icing. The twelve test groups allowed each surface type to be rotated into the six available positions of the spray chamber twice.*

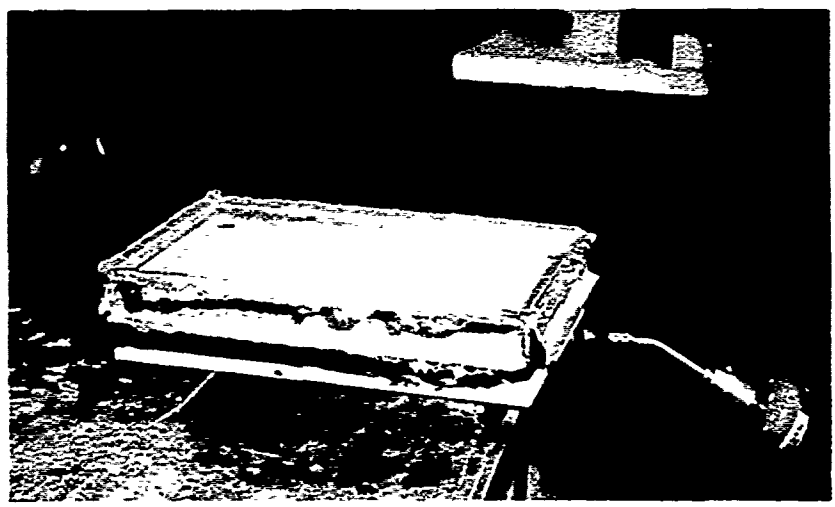

*Figure 7. Galvanized dams being removed by lightly heating them with a propane torch.*


*Figure 8. Sample edges being trimmed using a radial arm saw with a carbide-tipped blade.*

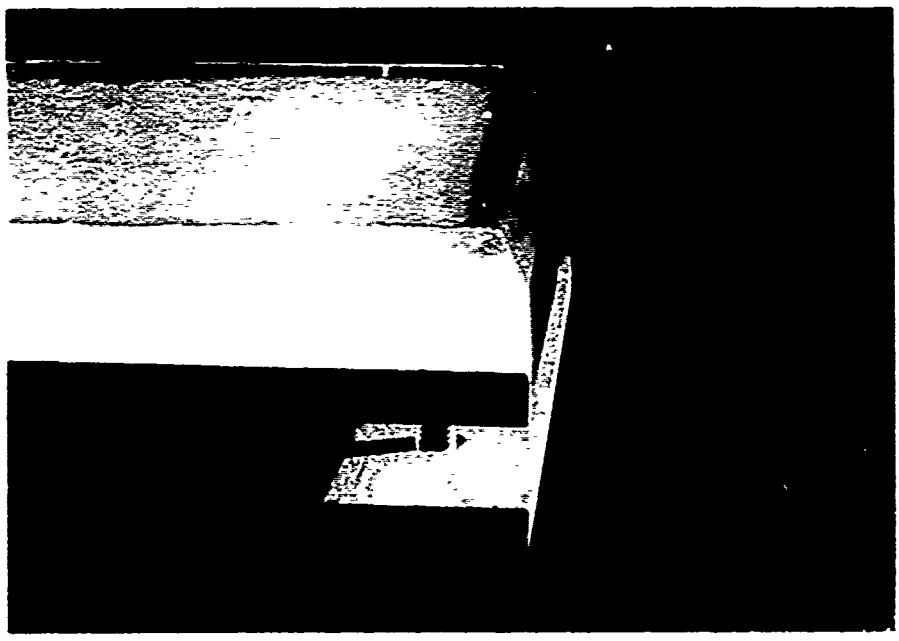

*Figure 9. Loading edge of a trimmed sample.*

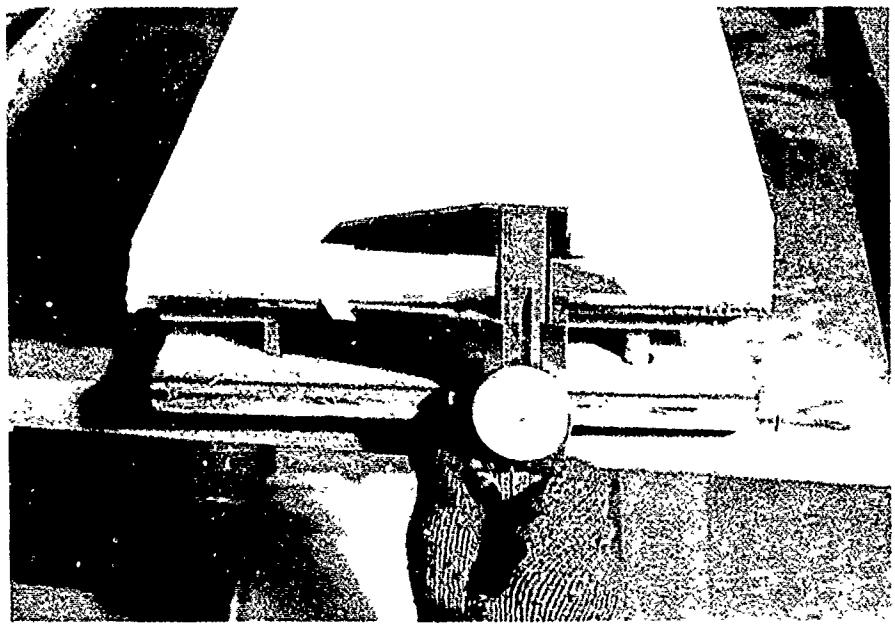

*Figure 10. Ice thickness being measured at one of three points on the loading end.*

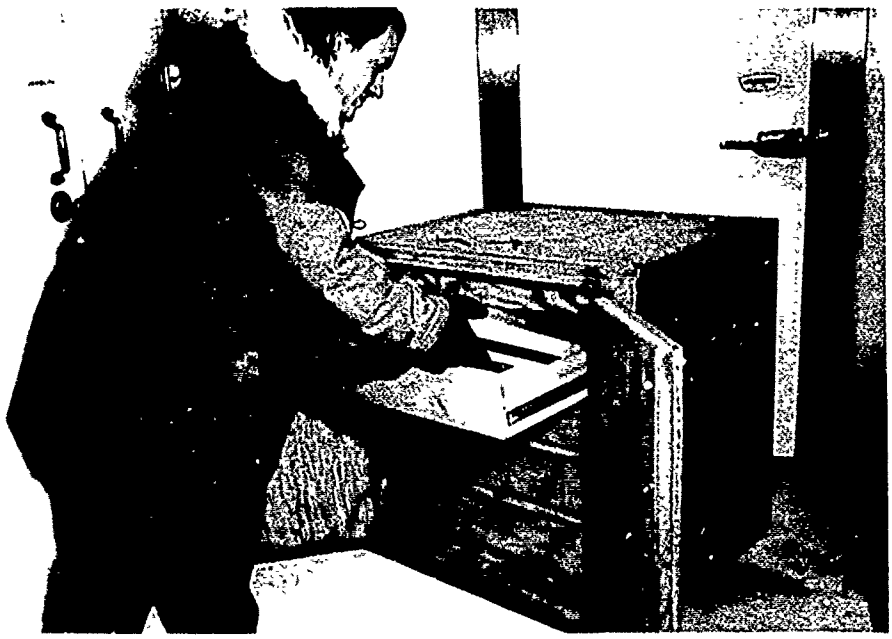

*Figure 11. Samples being transported between spray, preparation, and shearing areas on bubble-pack in an insulated box.*

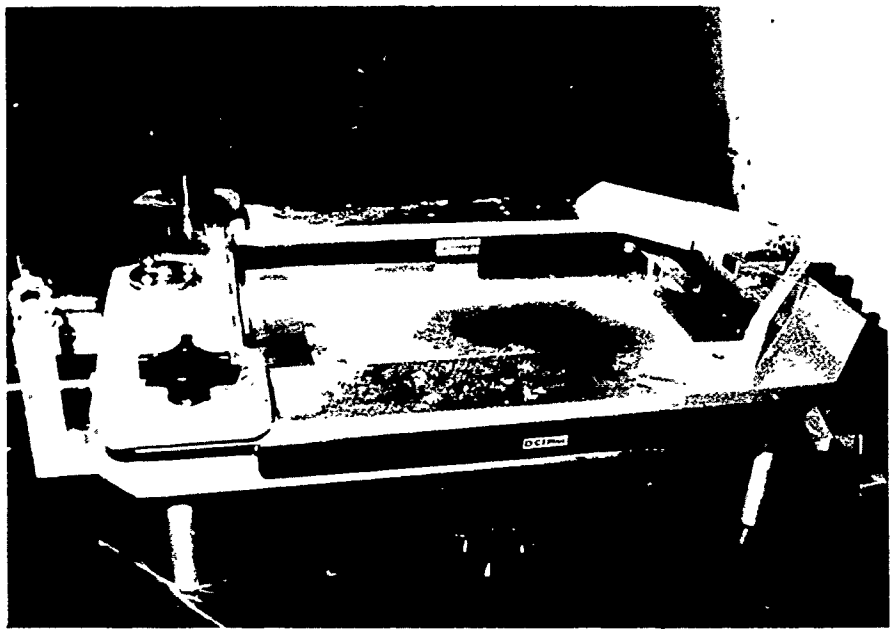

*Figure 12. Shear fixture. Loading direction is from left to right.*

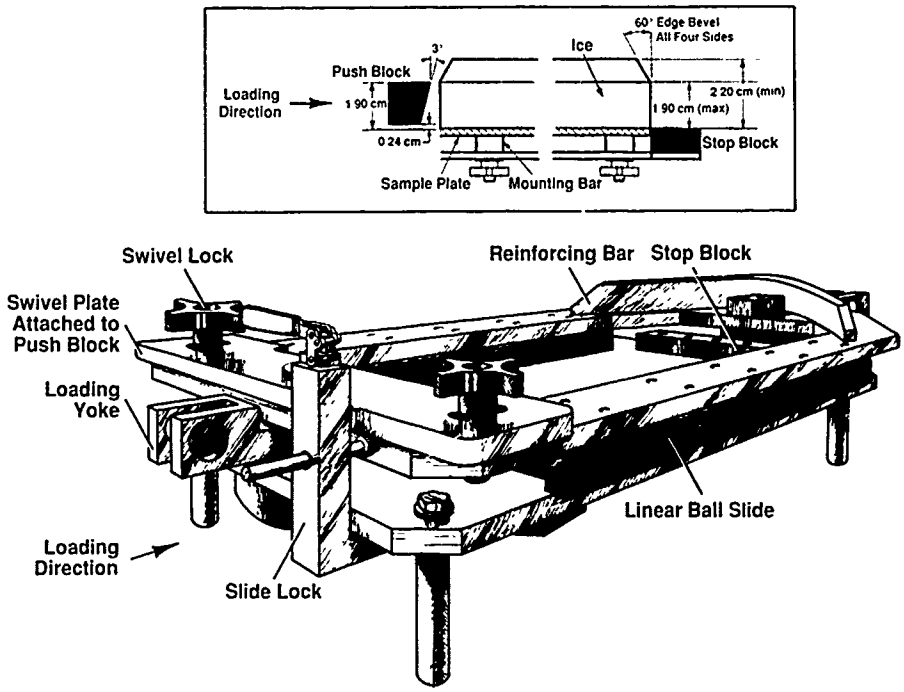


*Figure 13. Shear fixture and schematic presentation of the load application.*

## Shear fixture

An apparatus was designed and constructed for the experiment that fixed a sample plate and applied a shearing force at the ice/coating interface. The shear fixture (Fig. 12) consists of a sliding frame attached to a stationary base via two parallel precision linear ball slides. A sample is loaded into the shear fixture base and lightly held against a stop block by lock knobs turned onto the threaded studs of the mounting bars. Note, in Figure 13, that the top of the stop block is flush with the test surface of the sample plate. The plate is held fast while the shear force is imparted to the ice by a push block on the sliding frame. The top of the ice at the loading edge is beveled so that the thickness of its vertical face is less than the 1.9-cm height of the push bar. In addition, the push block can be swiveled on a center pivot to allow maximum alignment and surface contact with the ice (Fig. 14). Once this alignment is made, the swivel plate is locked into this position for the shear test.

Preliminary tests of shearing saline ice from steel and aluminum plates yielded surprisingly low adhesion values compared to those found in the literature (Oksanen 1982). It was speculated that the ice may have experienced peeling failure that would likely require lower forces (Sayward 1979). To counteract this possibility, a 3° bevel was subsequently machined into the push block to apply a slight downward component to the horizontal shear force. At the same time, the decision was made by the program sponsor to switch to freshwater ice adhesion testing. Although higher adhesion values resulted from these changes, shortage of time prevented a more thorough investigation of the interaction between the push block and the ice. The results pre-

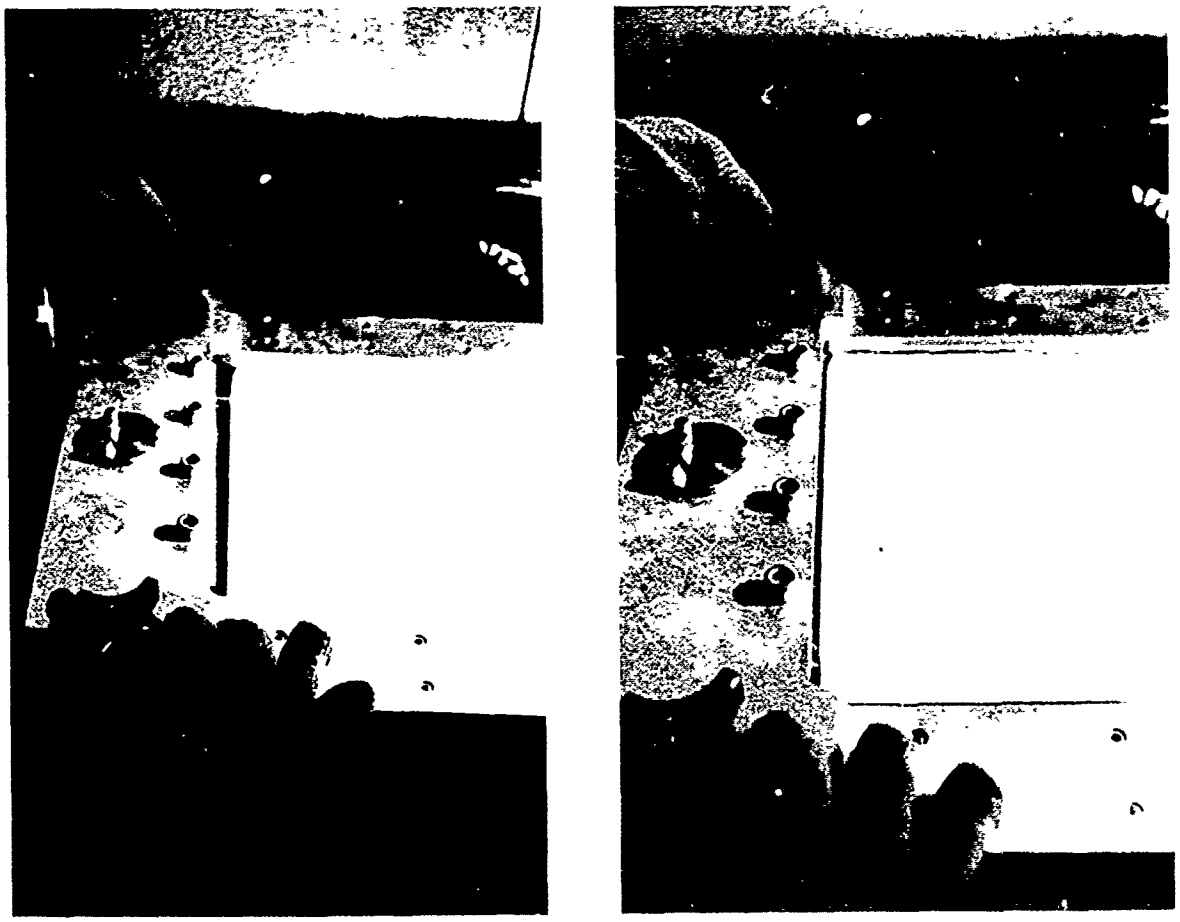

*a. Before alignment.*

*b. After alignment.*

*Figure 14. Rear section of the sliding frame that carries the push block swivels on a center pivot. This allows maximum alignment and surface contact of the push block with the ice. The push block is then locked into this aligned position for the shear test.*

sented here were obtained using the fixture with the beveled push block.

It is further speculated that unrealistically high salinity in the ice grown for our preliminary experiments may also have contributed to low adhesion values. Makkonen (1987) formulated the following theoretical equation for spray ice salinity, $S_i$:

$$S_i = \frac{0.26}{1-0.74n} S_w \quad (1)$$

where $S_w$ = salinity of the spray water

$n$ = the freezing fraction (ratio of spray volume accreted to the spray volume delivered).

Under dry growth conditions, where all of the spray delivered to an icing surface is frozen and there is no runoff ($n = 1$), the spray ice salinity would equal that of the spray water. However, the salinity of the ice approaches 26% of the salinity of the spray water under increasingly wetter growth conditions (as $n$ approaches 0). In the limit, seaspray at 35 ppt saline would theoretically produce ice accretions with a salinity of 9 ppt. Actual measurements have shown natural seaspray ice to be approximately 10 ppt saline (Sackinger 1985). Post-test analysis revealed that the bulk salinity of our accreted ice averaged 28 ppt. It appears that our method of ice growth using the galvanized steel dams inhibited natural brine drainage and desalinization.

**Testing machine**

The loading device used for these tests was CRREL's universal materials testing machine (Richter-Menge et al. 1986). It has a high force capability, high inherent stiffness, and delivers rapid response from a closed-loop, electrohydraulic fluid system. The main frame has a working capacity of 2.2 MN and a choice of hydraulic actuators delivering a quasi-static force capability of either 1.1 or 0.11 MN. For our tests, we used the large actuator, which was controlled through a 38-L/min servo valve and is capable of crosshead travel speeds up to 3.05 cm/s.

The machine has integral sensors for force and displacement in addition to the ability to monitor external load cells and strain transducers. Crosshead speed was controlled by programming the actuator to respond via closed-loop feedback to the integral displacement transducer. Load and displacement measurements were recorded at 20-ms intervals while the crosshead was displaced at a constant rate of 0.0381 cm/s during the test. Resolution of the total load was ± 44 N.

The testing machine is situated in a warm room and has a temperature-controlled test box mounted in its main frame to enclose the sample during the shear test (Fig. 15). The box is cooled by a cascade refrigeration

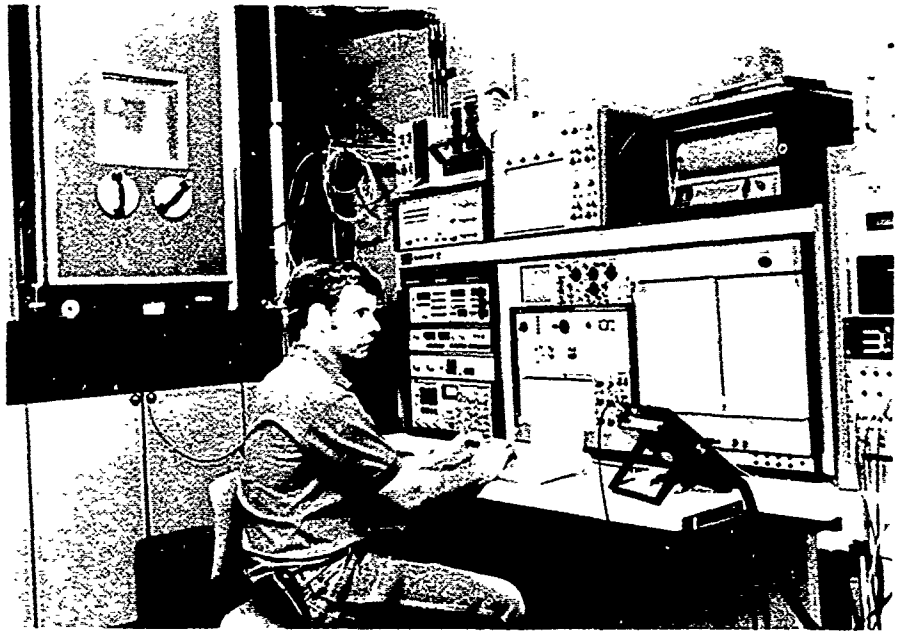

*Figure 15. Materials testing machine: test box and control console.*

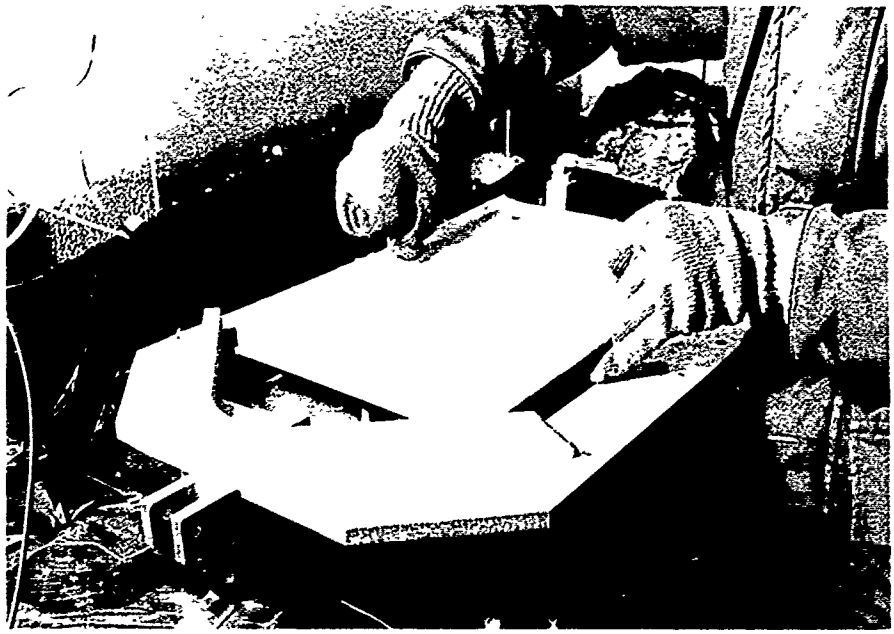

*Figure 16. Sample being individually loaded into the shear fixture and held in place with locking knobs turned onto the threaded studs that protruded through the bottom of the fixture.*

system capable of maintaining temperatures down to –50 ± 1°C.

**Sample shear testing**

On ·e a sample was mounted into the shear fixture (Fig. 16), the entire fixture-and-sample assembly was wrapped in an insulated jacket to maintain its temperature while transferring it from the coldroom to the test box (Fig. 17 and 18). While the door of the test box was open to load the assembly into the actuator of the testing machine, the cold air was displaced by warm room air. Once enclosed in the test box, the sample could be

*Figure 17. Shear fixture with sample was wrapped with an insulated jacket before loading into the testing machine.*

*Figure 18. Insulated jacket ensured that the sample remained at –10 ± 1°C during the transfer from coldroom to test box.*

accessed from the warm room through small hand ports. The test box air temperature was allowed to stabilize at –10°C before using the hand ports to remove the jacket and attach a displacement transducer to the shear fixture. This additional transducer provided an alternate measurement of ice deformation rate during each test in the event that the integral displacement transducer on the load actuator failed. After the test (Fig. 19), the assembly was jacketed and removed to the coldroom to photograph the fracture pattern and to visually inspect the ice and plate surface conditions. Traces of frost or ice remaining on the plate after the test were documented. The uniformity of the ice/substrate bond was observed from the underside smoothness of the shorn ice. The presence of air voids at the interface would have indicated nonuniform ice coverage or incomplete bonding. In general, complete and uniform bonding between the ice and the test surface was observed in all samples.

All production, preparation, and shearing procedures were performed on each test group in the order in which the samples were placed in the spray chamber so that processing time could be eliminated as a variable in the tests.

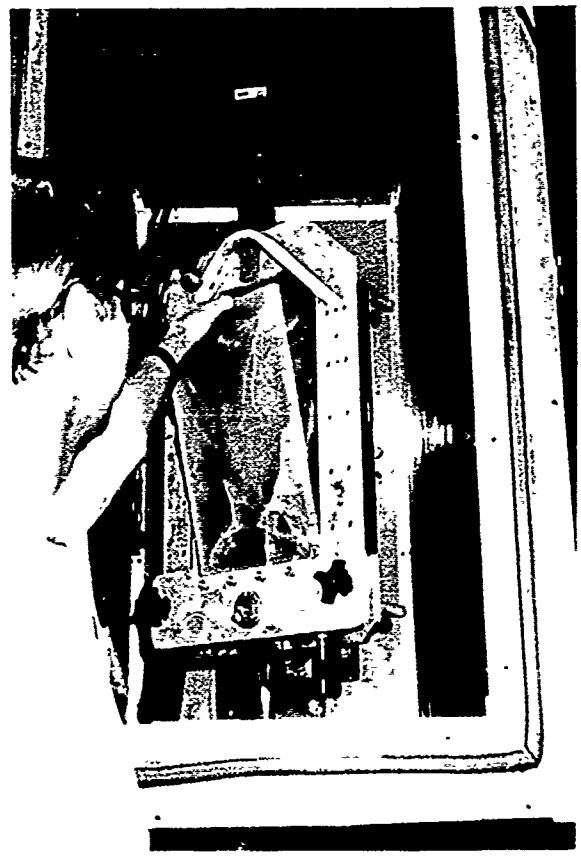

*Figure 19. Sample after shear test. Insulated jacket has been removed to better show the test configuration.*

## RESULTS

### Spray icing

After much experimentation, the ice growth regime that was selected for sample production employed a

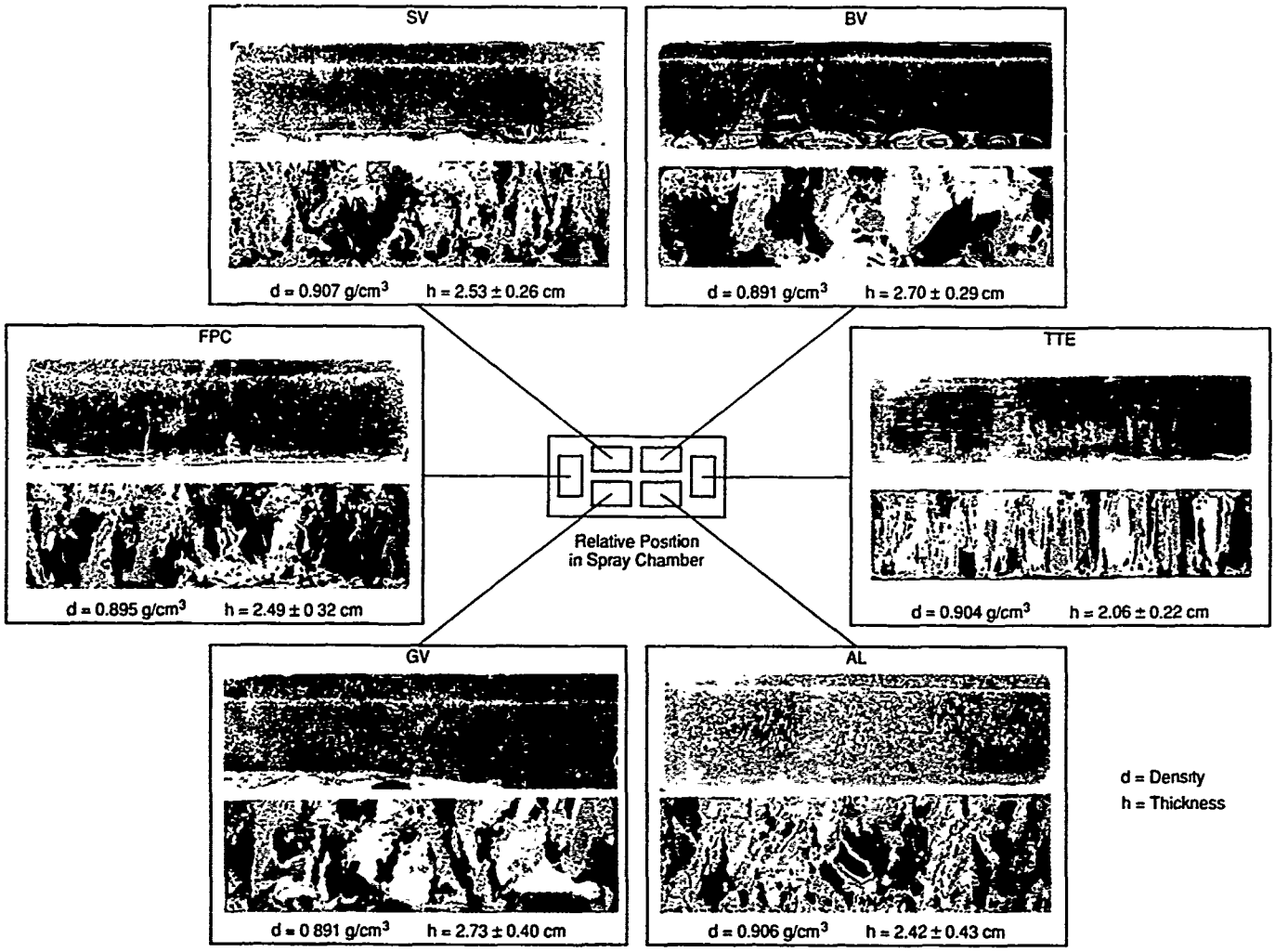


*Figure 20. Vertical thin sections of the samples from test group 620 and the positions the samples occupied in the spray chamber. The ice/plate interface is at the bottom of the photographs. Densities were measured for test group 620 only. Thicknesses are the mean and standard deviations of the 12 ice layers grown in that particular chamber location.*

repetitive blow, pause, and spray cycle of 180, 4, and 3 seconds, respectively. The long blow mode allowed most of the deposited water to freeze prior to the addition of more water. Water was sprayed onto the samples to build up the ice at a rate of approximately 0.6 cm/hr and all ice covers were grown to 2.49 ± 0.39 cm thick. This produced an ice type that was primarily *glaze* in character, i.e., slowly frozen ice that is relatively bubble-free and of high density.

Figure 20 shows vertical thin sections (bottom edge of thin section was in contact with the plate) that were cut from the ice covers of test group 620 after shear testing was performed. Each section was taken near the center of the test plate. The top photographs, as a group, show that the ice was nearly clear with only a few small bubbles distributed in the ice, away from the interface. The bottom photographs are of the same thin sections placed between crossed Polaroid sheets and show that the orientation of the crystals within each sample is not uniform. All samples in the figure, with the exception of the TTE sample, are similar in appearance with respect to crystal structure. These samples have a range of crystal shapes, from nearly spherical to directionally elongated. The distribution and orientation of these crystal types is random. The TTE sample differs due to the presence of a preferred crystal orientation. Crystals in this sample exhibit vertical elongation. This variation in crystal structure is likely associated with placement within the spray chamber. The TTE sample was placed in the chamber location that typically produced the thinnest ice cover. The grain size ranges from 2 to 4 mm in the TTE sample, to between 5 and 10 mm in the Gray

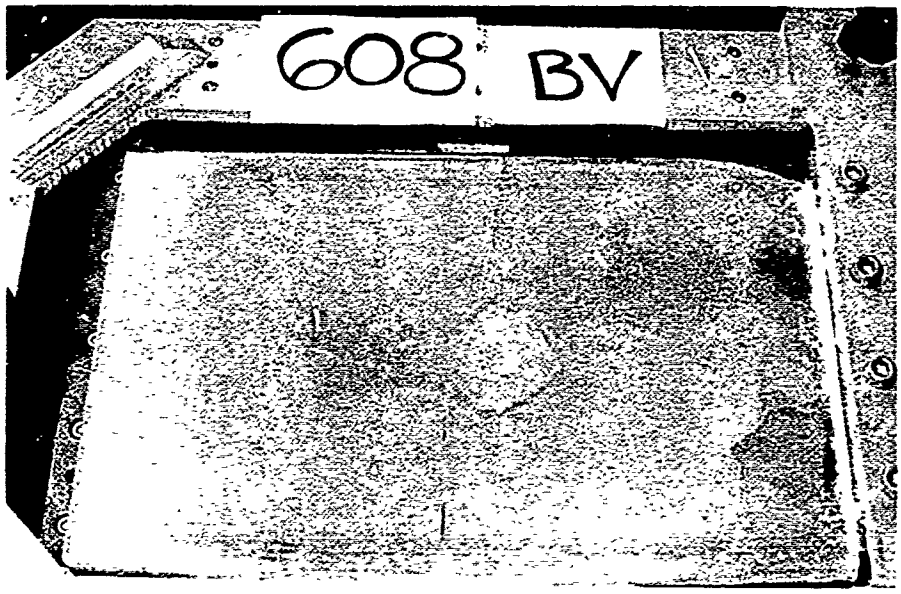


*Figure 21. Typical sample with a freezing-relief fracture near its center and a shear fracture pattern that intersects with it. Loading direction is from R to L. Loading edge shows typical crushing and flaking caused by the beveled push bar.*

and Black Vellox samples. All samples have distinct layering, visible in both photographs, near the top surface. The FPC and Vellox samples all have additional layering near the ice/substrate interface.

The ice densities of the samples from test group 620 were measured by mass/volume technique and found to range from 0.891 to 0.907 g/cm$^3$. The measured density for each sample is shown in Figure 20, as is the mean and standard deviation of the ice thickness for the 12 samples that were grown in that specific chamber location. Based on visual appearance, these samples were not atypical and their mean density of 0.9 g/cm$^3$ was assumed to be representative for all test groups.

In brief, this analysis has shown that structural differences in the ice covers between samples of a test [illegible] were readily apparent. It is assumed, given our strict adherence to a consistent ice growing procedure and by rotating the various surface types through the six available chamber positions, that the effect on adhesion strength due to ice structure has been randomized. More will be said later concerning the effect of ice thickness variation on our measured shear strengths.

If the freezing rate was not rapid enough, a reservoir of excess water became trapped within the ice. After the sprayer was turned off, the unfrozen water became concentrated near the center of the ice cover as the sample cooled from the outside inward. Complete water-to-ice phase change resulted in a "freezing relief" swelling with localized fractures in the swollen area. This phenomenon occurred to varying degrees in 20 of the 72 samples. Figure 21 shows a typical example of freezing relief and a shear test fracture pattern that intersects with it.

Average thickness for all six samples in each test group was plotted as a function of time with the temperatures that were recorded during each growth period. The temperature trace for a typical ice growth period is shown as Figure 22. Similar growth temperature records for all test groups are in Appendix B. Air temperatures were very stable throughout the growth period. However, the water temperature increased gradually due to the small water reservoir capacity (approximately 100 L) and heating caused by the submersed circulation pump. If icing period 530 is neglected, the mean temperature in the reservoir at the start of the icing periods was 7.9 ± a standard deviation of 1.6°C and at the end was 11.3 ± 1.0°C, a 3.4°C increase in temperature. For icing period 530, the reservoir temperature experienced a 2.0°C decrease after starting abnormally high (22°C) because the chamber had been left operating in a defrost mode over the weekend prior to icing. A temperature increase of 6.0°C was experienced by test group 612 during icing due to nozzle freezeup and the greater length of time necessary to achieve the desired ice thickness. However, the fracture behavior and shear stresses measured for the samples from these two test groups were not noticeably different from those of other test groups.

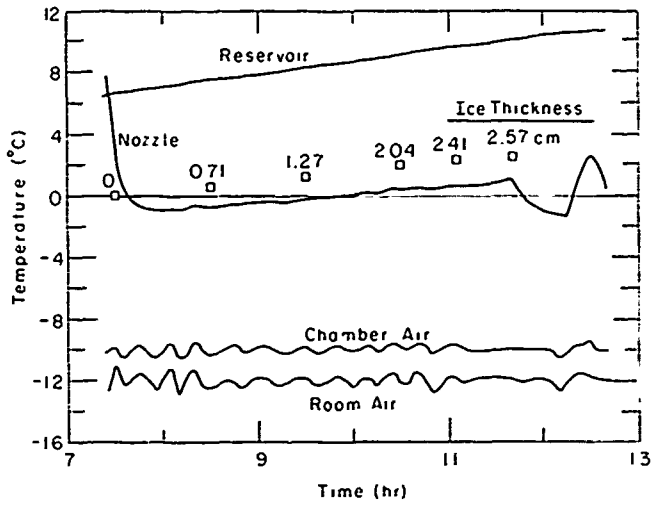


*Figure 22. Typical temperature and ice thickness record during an ice growth period.*

Because the nozzle thermocouple was placed on the outside of the nozzle and not in the water stream, it only indicated if and when nozzle freezeup occurred. Short duration peaks in the nozzle temperature occurred when the spray chamber was put into a standby mode and ice thickness measurements were performed. More prolonged shifts indicate either nozzle freezeup and consequent efforts to thaw, the application of more insulation to prevent freezeup, or a change in the location of the sensor.

**Shear testing**

Appendix C contains the loading histories for the 64 successful tests (8 out of the original 72 were discarded as failed tests). In approximately half the tests more than one peak in the loading trace occurred. These multiple peaks resulted from local failures in the ice cover before the general and complete failure at the ice/coating interface. Actual examples of the various types of failure observed are shown in Figure 23 and are defined as follows:

Type I — A single peak in the load trace.

Type II — Two peaks in the load trace.

Type III— Three peaks in the load trace.

Type IV— Four or more peaks in the load trace.

One cause of multiple stress peaks was flaking of the upper edge of the ice in direct contact with the beveled push block. Since the face of the ice was vertical and that of the push block was beveled 3° from vertical, the top corner of the loaded ice edge would typically be crushed early in the test. The contact area between the ice edge and the push block increased as the block moved forward and crushing proceeded. The amount of crushing and local fracturing of this front top edge that occurred prior to general ice failure was a function of the overall bond strength of each sample. Notice, in Figure 21, the flaked top edge along the right side of sample 608-BV50 caused by the push block bevel. This is an extreme example of the crushing action that occurred along the loading edge of many samples during the shear test. The extensive ice crushing of this particular sample correlates well with its high shear strength. It should be noted that this sample produced the Type IV failure example of Figure 23. It is surmised that the two small peaks early in the test were the result of edge crushing. The third peak may have been caused by the obvious transverse fracture through the middle of the ice sheet. Finally, the general failure at the interface produced the largest and last peak. Appendix D contains post-test illustrations of fracture patterns for the 64 tests.

The coatings were compared based on the maximum stress peak attained during the shear test. For example, four peaks occurred in the load trace for sample 608-BV50, at 13.6, 18.9, 104.8, and 127.4 kPa, respectively. The largest peak, 127.4 kPa, was selected for comparison with the other samples. Table 1 lists the shear tests according to coating and failure type. The number in parentheses following each sample name refers to where its peak stress ranks in increasing magnitude relative to the other 63 tests. This rank order is used later in our statistical analyses of the test results.

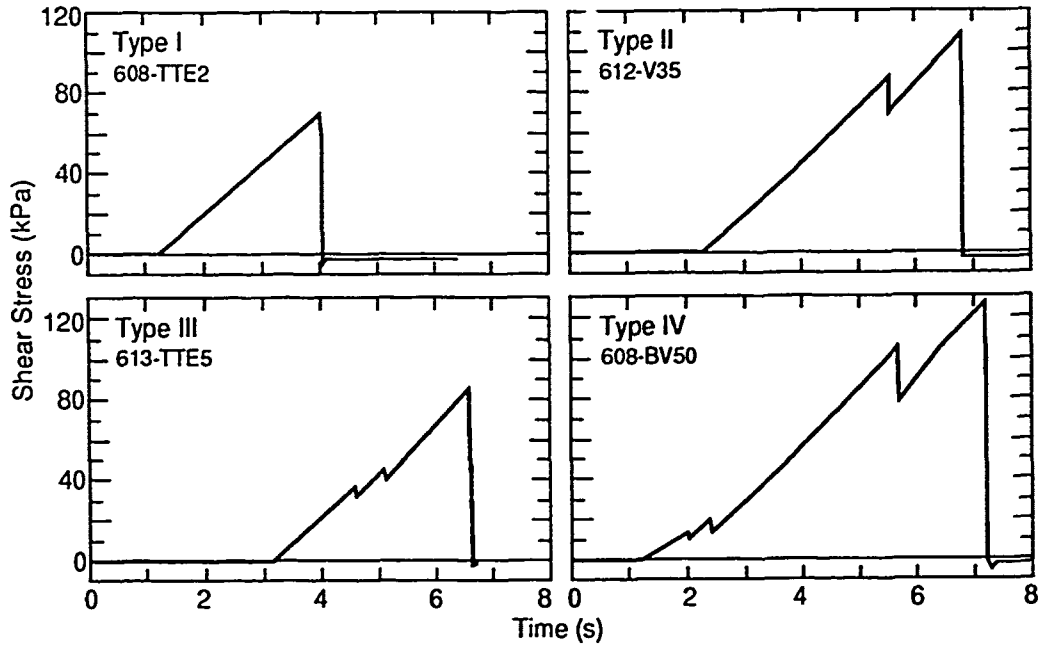


*Figure 23. Loading histories of actual samples illustrating the four types of fracture behavior.*

Type I or II failure occurred in 48 out of 64 of the tests. It should be noted that TTE had the largest number of samples that failed with Type III or IV behavior (5 out of 11). However, the peak stresses measured for these samples averaged 73.9 ± 13.6 kPa (mean ± standard deviation) as compared to 71.6 ± 15.1 kPa for the entire TTE group. The similarity of the means and standard deviations indicates that the maximum stress was not greatly affected by additional peaks in the loading history.

The samples with freezing relief expansion are also indicated in Table 1. Intuitively, we would expect the shearing behavior and magnitude to be affected by the presence of freezing relief expansion. In terms of behavior, there was no discernible difference in the stress–time curve of samples with shear fractures that intersected relief-swollen areas and the samples without intersecting fractures. The samples with freezing relief expansion were quite evenly distributed between the four failure types. Also, 20 samples suffered freezing relief expansion and of these, nine showed no detectable shear fractures intersecting the swollen areas. Shear fractures intersecting swollen areas appears to be random. Regarding stress magnitudes, of the nine samples without intersecting fractures, eight had shear strengths lower (by an average of 22%) than the mean values of their particular surface type. Of the eleven samples with intersecting fractures, nine had shear strengths higher (by an average of 21%) than their means. Despite the observation that the stress magnitudes may have been affected, our analysis of coating performance does not take this into account. We compared the maximum stress measured in each test regardless of failure type and/or the presence of freezing relief.

Figure 24 is a plot of shear strength vs ice thickness. The shear strengths were normalized by dividing each test value by the mean value of its particular surface type. For example, the peak stress measured for sample 608-BV50 is divided by the mean stress of the nine successful Black Vellox tests to obtain the normalized shear strength:

Peak stress for individual sample = 127.4 kPa

Mean stress for the coating group = 119.2 kPa

$$\text{Normalized shear strength} = \frac{127.4}{119.2} = 1.07.$$

Neither ice thickness at the center of the plate nor the average of three measurements of the height of the vertical loading face correlates with normalized shear strength. It is apparent from Figure 24 that our test method is not sensitive to ice thickness. Therefore, the unavoidable thickness variations that resulted from the spray icing procedure were not an apparent factor in our test results.

**Table 1. Shear failure type for all samples listed by coating. First three digits in the sample name identify the test group, and last digits identify the plate number. Ascending rank of peak shear values for the 64 successful tests appear in parentheses.**

| | *Aluminum* | *TTE-490* | *FPC* | *Std. Vellox* | *Gray Vellox* | *Black Vellox* |
|---|---|---|---|---|---|---|
| TYPE I | 525-A1 (2) | 606-T3 (33) | 601-F22 (41) | 613-V34*† (53) | 606-G48 (42) | 614-B54* (61) |
| | 601-A2 (39) | 607-T7 (34) | 606-F21*† (60) | 619-V29 (54) | 612-G38*† (43) | 619-B49 (47) |
| | 606-A2 (24) | 608-T2 (16) | 613-F18* (19) | 620-V25 (40) | 613-G42*† (35) | |
| | 607-A3 (23) | 614-T1* (1) | 614-F17 (27) | | 615-G39 (10) | |
| | 619-A5 (49) | | 615-F14*† (63) | | 619-G46 (36) | |
| | | | 619-F24 (28) | | 620-G37* (8) | |
| TYPE II | 530-A1 (26) | 612-T9 (5) | 530-F23 (46) | 530-V27 (45) | 601-G43 (7) | 530-B58 (56) |
| | 612-A3*† (9) | 619-T8*† (12) | 607-F20 (13) | 601-V33 (14) | 607-G47*† (48) | 612-B60 (52) |
| | 614-A5 (25) | | 612-F15 (29) | 612-V35*† (50) | 614-G41 (57) | 620-B51 (64) |
| | 615-A6 (58) | | 620-F13 (62) | 614-V28* (17) | | |
| | 620-A6 (51) | | | 615-V30 (37) | | |
| TYPE III | 608-A4 (4) | 525-T6 (22) | 525-F16 (21) | 606-V32 (15) | 530-G44* (20) | |
| | 613-A4 (11) | 613-T5*† (32) | 608-F19 (6) | | | |
| | | 615-T4 (18) | | | | |
| TYPE IV | | 530-T10* (3) | | | 608-G45* (30) | 601-B57 (55) |
| | | 620-T11 (31) | | | | 606-B56* (44) |
| | | | | | | 608-B50*† (59) |
| | | | | | | 613-B59 (38) |

*Pre-test freezing relief swell in ice.
†Shear test fractures intersect freezing relief swell.

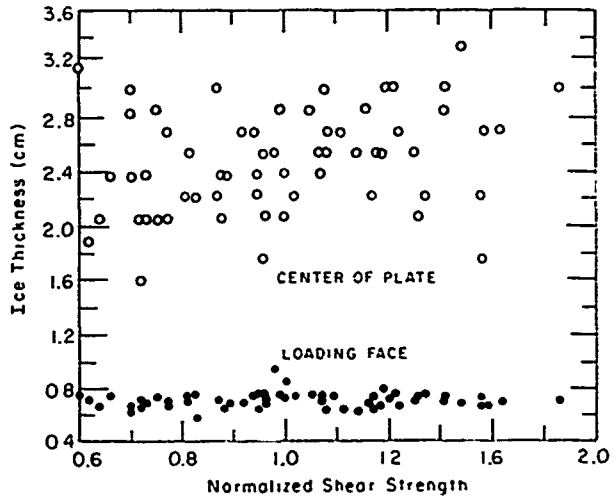


*Figure 24. Plot of shear strength vs ice thickness shows no correlation. Our shear test results were not affected by ice thickness.*

## DISCUSSION

There is a multitude of literature on previous ice adhesion work, yet comparisons are difficult to draw due to differences in test configuration, ambient conditions, ice type, test surfaces, and force application. Our test method employed a sample displacement rate that was higher by at least an order of magnitude than many previous adhesive shear studies that utilized constant displacement rate. The rates that were used in six such studies are listed below:

| | *Displacement Rate (cm/s)* |
|---|---|
| Druez et al. (1986) | 0.043 |
| Lyrra et al. (1986) | 0.00083 |
| Oksanen (1982) | 0.00017 and 0.0017 |
| Jones and Gardos (1972) | 0.0042 and 0.042 |
| Savelyev et al. (1972) | 0.003 |
| Jellinek (1960) | 0.041. |

We chose a rate of 0.0381 cm/s to ensure brittle failure of the ice. The method produced virtually 100% ice removal in every test, which eliminated analysis problems associated with cohesive failure and partial ice removal. Bits of ice covering less than 1% of the total surface area remained on the plate following ice release in only 7 out of 64 successful tests. This allowed the stress calculations to be obtained by dividing all the peak loads by the same surface area (871 $cm^2$).

The Standard and Black Vellox samples, in 16 out of 18 cases, had extensive areas of frost-like residue remaining on the plate after the shear test (Fig. 25). This was an artifact perhaps of the manner in which the ice formed. Vellox repels water droplets due to its microscopic pore structure. Due to surface tension, the droplet cannot penetrate into the Vellox pores and a barrier of air remains between it and the test surface. The droplets tend initially to "bead" and roll off inclined surfaces. This behavior is referred to by Sayward (1979) as the "gaseous plastron effect." Surface tension produces droplet-to-Vellox contact angles in excess of 140° according to the manufacturer's literature. This water repellency feature was circumvented by our arrangement of horizontal plates with dams to trap the spray, which ensured an equal rate of ice formation on all samples. On all Vellox samples, the droplets would roll about freely or pool with other droplets before freezing, unless they came into contact with the walls of the dam. Usually, freezing occurred immediately around the edges and advanced inward as the ice attracted the freely rolling droplets. Figure 26 shows a test group in the early stages of icing and illustrates this point. Water beaded somewhat on the FPC surfaces and "sheeted" fairly evenly (low contact angle) on the TTE and AL samples. Curiously, the Gray Vellox samples exhibited no residual post-test frost-like residue even though ice formed on them in a manner similar to the other Vellox types.

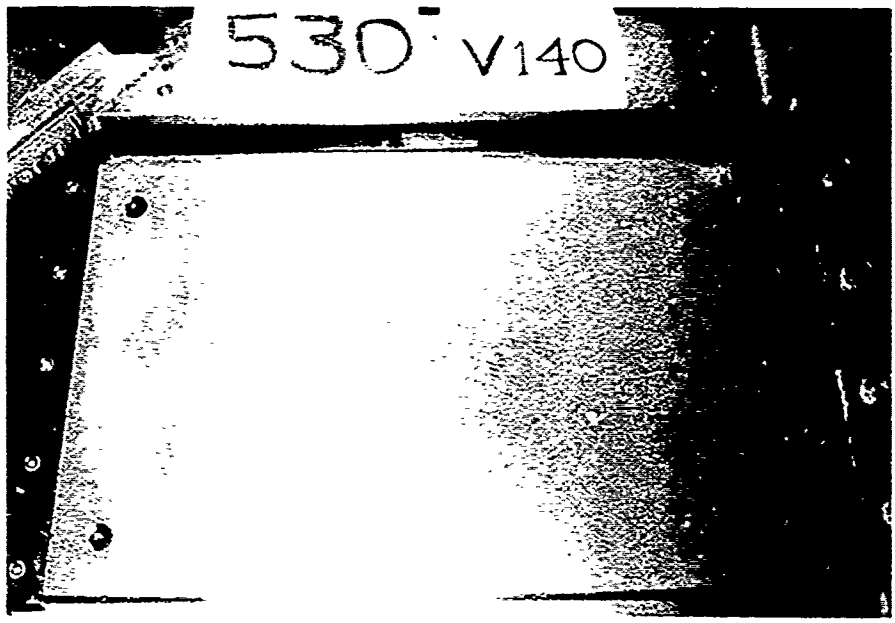


*Figure 25. Standard Vellox sample after the shear test showing traces of frost-like residue on the plate.*

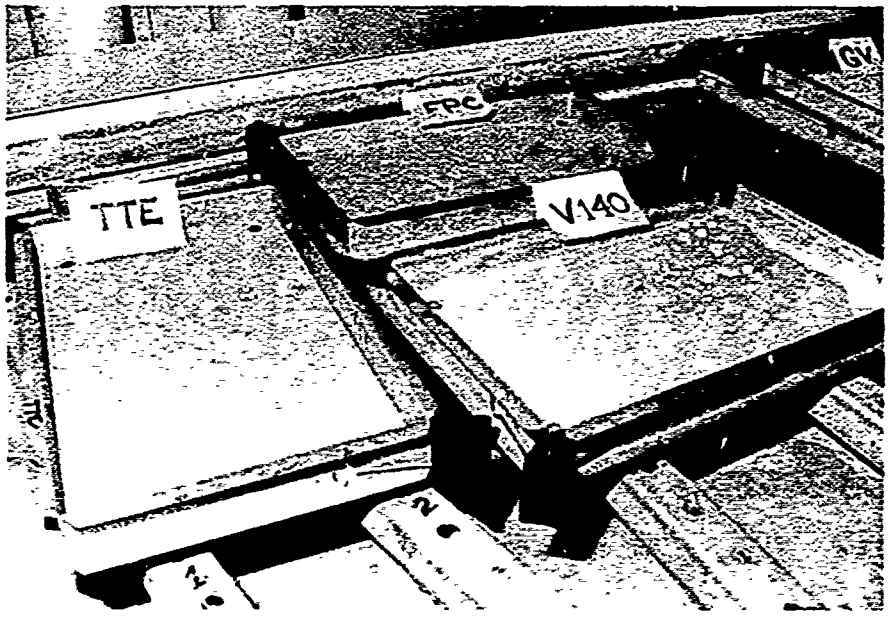


*a. Samples under left spray nozzle.*

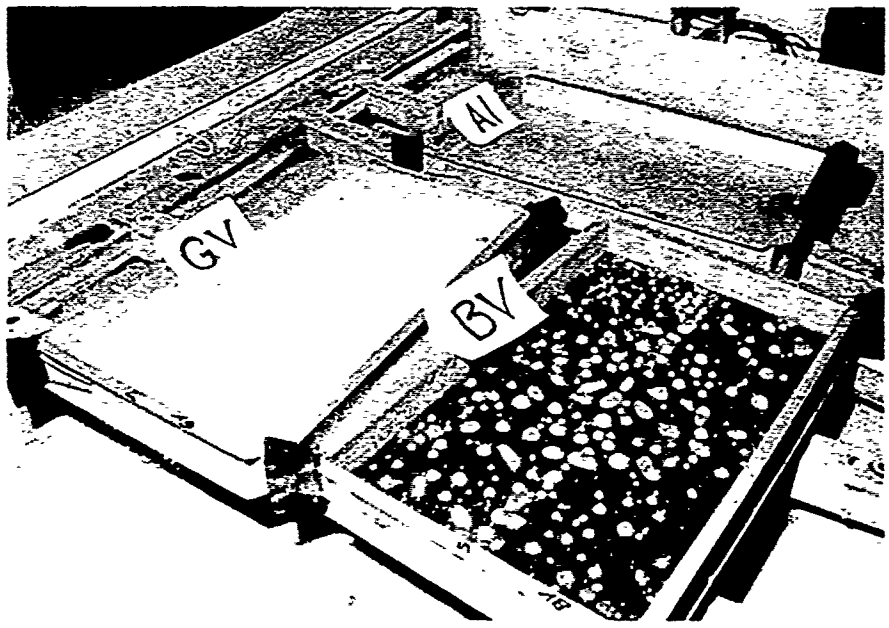


*b. Samples under right spray nozzle.*

*Figure 26. Test group in early stages of spray icing.*

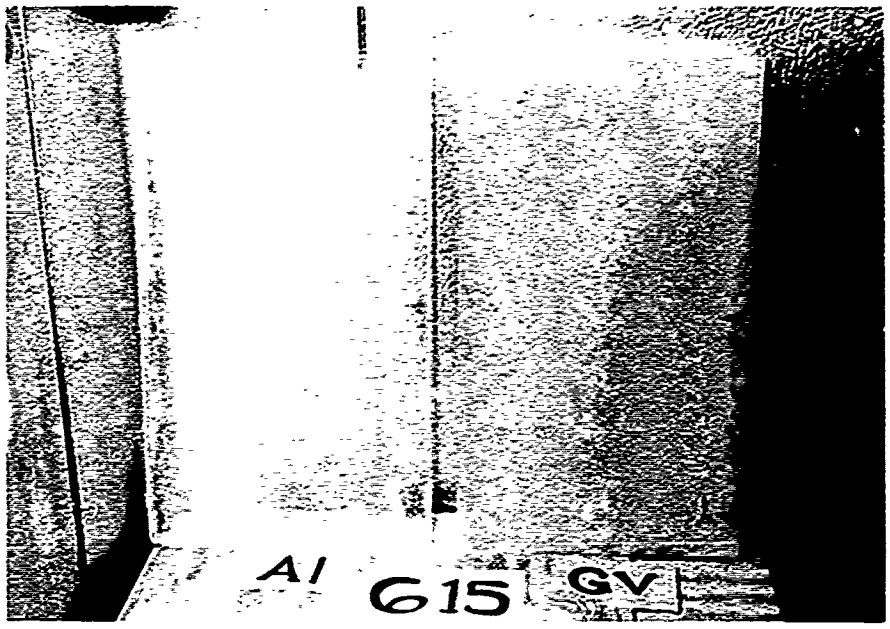


*Figure 27. Ice that was shorn from Aluminum and Gray Vellox samples, showing the large amount of coating that was always removed with the ice from the Vellox samples.*

Another observation regarding Vellox surfaces was the massive amount of coating that was removed along with the ice during shear testing. Figure 27 shows the ice from an aluminum sample next to the ice from a Gray Vellox sample. The translucence of the AL ice, due to fine bubbles, is in vivid contrast to the opaque, powder-covered surface of the GV ice. This behavior raises the question of coating durability and whether adhesive strength would change dramatically over repeated ice/shear cycling. Since our program tested each sample only once, we can only suggest that the durability of Vellox coatings may be worth studying more closely.

The test program was designed to answer whether any of the candidate coatings would exhibit lower ice adhesion values than the standard Navy deck paint, TTE-490. In fact, our results indicate that none of the coatings effectively reduced adhesion strength for ice. Results of the 64 shear tests and summary statistics for each surface type are presented in Table 2. ("Plate no." in the table refers to the number that was assigned to the sample by DTRC.) All the coatings had higher mean shear values than the two controls, TTE-490 and aluminum. Based on the mean peak loads, the various surface types rank from lowest to highest in the following order:

| Surface type | TTE | AL | GV | FPC | SV | BV |
|---|---|---|---|---|---|---|
| Rank | 1 | 2 | 3 | 4 | 5 | 6 |
| Stress (kPa) | 71.6 | 82.1 | 87.9 | 92.8 | 94.4 | 119.2 |
| Std deviation (kPa) | 15.1 | 22.6 | 20.0 | 24.5 | 19.0 | 16.5 |

Three previous adhesion studies utilized shear rates comparable to ours and obtained results similar to ours in terms of shear strength magnitudes. Though not absolutely comparable due to differences in test method and ice type, the tests of Druez et al. (1986) measured the adhesive strength of ice grown in a wind tunnel to aluminum rods using a shear rate of 0.043 cm/s. His shear value for ice at –10°C with a density of 0.8 g/cm$^3$ was 108 kPa with a standard deviation of 20 kPa. Jones and Gardos (1972) reported 63 kPa for sandblasted steel at –54°C using a displacement rate of 0.042 cm/s. Jellinek (1960) reported a mean adhesive strength of 69.6 ± 18.4 kPa for ice bonded to fused quartz at –4.5°C using a shear rate of 0.041 cm/s. Our mean bond strengths were of the same order of magnitude as these values, yet our range, from 71.6 to 119.2 kPa, was surprisingly small given the variety of surfaces tested. Additionally, given standard deviations of the means ranging from 15.1 to 24.5 kPa, it was especially important to test the results for statistical significance.

The significance tests were conducted assuming the null hypothesis, $H_0$, to be "coating 1 has the same affinity for ice as coating 2." In order to reject the null hypothesis in favor of the alternate hypothesis, $H_1$ (i.e., the mean ice bonding strength of coating 1 is less than that of coating 2), the probability must be very low for obtaining identical shear means. The small sample size (less than 15 per surface type) and the possibility of unequal variances or non-Gaussian sample distributions

**Table 2. Shear test results. Peak stresses are in kilopascals. %SDEV is the standard deviation of peak stress divided by the mean stress and expressed in percent (sometimes referred to as "relative percent deviation"). Missing values indicate an unsuccessful test.**

| | *Aluminum* | | *TTE-490* | | *FPC* | | *Std. Vellox* | | *Gray Vellox* | | *Black Vellox* | |
|---|---|---|---|---|---|---|---|---|---|---|---|---|
| *Test group* | *Plate no.* | *Peak stress* | *Plate no.* | *Peak stress* | *Plate no.* | *Peak stress* | *Plate no.* | *Peak stress* | *Plate no.* | *Peak stress* | *Plate no.* | *Peak stress* |
| 525 | 1 | 50.9 | 6 | 76.9 | 16 | 74.9 | 26 | — | 40 | | 52 | — |
| 530 | 1 | 80.2 | 10 | 52.0 | 23 | 105.6 | 27 | 104.9 | 44 | 72.9 | 58 | 119.7 |
| 601 | 2 | 97.6 | 12 | — | 22 | 100.6 | 33 | 68.2 | 43 | 61.5 | 57 | 119.6 |
| 606 | 2 | 78.2 | 3 | 90.1 | 21 | 128.0 | 32 | 68.3 | 48 | 102.9 | 56 | 104.1 |
| 607 | 3 | 77.4 | 7 | 91.3 | 20 | 67.3 | 31 | — | 47 | 106.9 | 55 | — |
| 608 | 4 | 54.1 | 2 | 68.8 | 19 | 59.8 | 36 | — | 45 | 83.3 | 50 | 127.4 |
| 612 | 3 | 61.8 | 9 | 58.7 | 15 | 81.7 | 35 | 109.4 | 38 | 103.7 | 60 | 114.3 |
| 613 | 4 | 63.0 | 5 | 85.6 | 18 | 71.7 | 34 | 114.4 | 42 | 95.3 | 59 | 96.7 |
| 614 | 5 | 79.0 | 1 | 43.0 | 17 | 81.0 | 28 | 70.8 | 41 | 121.4 | 54 | 128.6 |
| 615 | 6 | 125.5 | 4 | 71.1 | 14 | 131.8 | 30 | 96.1 | 39 | 61.9 | 53 | — |
| 619 | 5 | 107.2 | 8 | 66.1 | 24 | 81.3 | 29 | 118.3 | 46 | 95.5 | 49 | 106.2 |
| 620 | 6 | 109.8 | 11 | 83.9 | 13 | 128.9 | 25 | 99.6 | 37 | 61.6 | 51 | 156.4 |
| Mean | | 82.1 | | 71.6 | | 92.7 | | 94.4 | | 87.9 | | 119.2 |
| SDev | | 22.6 | | 15.1 | | 24.5 | | 19.0 | | 20.0 | | 16.5 |
| %SDev | | 28.7 | | 22.2 | | 27.6 | | 21.4 | | 23.8 | | 14.7 |
| No. of samples | | 12 | | 11 | | 12 | | 9 | | 11 | | 9 |

required that the statistical tests be nonparametric (Tashman and Lamborn 1979). Kruskal-Wallis and Mann-Whitney tests were chosen (Seigel 1956, Shaw and Wheeler 1985). These distribution-free tests permit the determination of significance, even though less is known about the sample population than is required for using parametric tests such as the *F*-test and Student's *t*.

The Kruskal-Wallis test is a group analysis of variance that shows whether there is significant difference between any of the six sample groups. The test showed with 97.6% confidence that there is a significant difference between at least two of the sample groups. Two-group comparisons were done using the Mann-Whitney test to isolate where the differences were.

The Mann-Whitney test produces the *U* statistic, which is identical to the Wilcoxon *W* statistic but differs in how it is derived (App E). We purposely avoided establishing coating rejection criteria and left those decisions to the program sponsor, DTRC. We have chosen instead to report confidence levels for our data. Table 3 shows the confidence level matrix derived from probabilities that were calculated by the Mann-Whitney tests (Norusis 1986). Each value in the matrix is the level of confidence that $H_0$ can be safely rejected in favor of $H_1$, and that coating 1 has a lower bond strength than coating 2. As shown in Table 3, the low confidence levels between FPC and SV (51%), GV and FPC (58%),

**Table 3. Confidence level matrix for coating preference (i.e., Coating 1 has lower bond strength than Coating 2) based on Mann-Whitney tests of peak shear values.**

| | *Coating 1* | | | | | |
|---|---|---|---|---|---|---|
| | *TTE* | *AL* | *GV* | *FPC* | *SV* | *BV* |
| Rank* | 1 | 2 | 3 | 4 | 5 | 6 |
| | *Coating 2* | | | | | |
| TTE | 0.0000 | | | | | |
| AL | 0.8265 | 0.0000 | | | | |
| GV | 0.9620 | 0.6526 | 0.0000 | | | |
| FPC | 0.9604 | 0.8672 | 0.5836 | 0.0000 | | |
| SV | 0.9874 | 0.8614 | 0.8149 | 0.5138 | 0.0000 | |
| BV | 1.0000 | 0.9988 | 0.9988 | 0.9754 | 0.9906 | 0.0000 |

* According to ascending mean shear values.

GV and SV (81%), indicate that the test program did not successfully resolve the order of preference for these three coatings. However, we believe the more significant finding to be that the standard Navy deck paint, TTE-490 performs most favorably under the test conditions. TTE-490 had significantly lower bond strength than all the other surfaces with greater than 96% confidence except for the aluminum control. The Mann-Whitney test indicated with only 83% confidence that the mean bond strength of TTE is lower than that of aluminum.

A clear trend from the analysis is that the three versions of Vellox have a higher affinity for ice than TTE. Further, Black Vellox has significantly higher adhesive strength for ice than all other surfaces with a minimum of 97% confidence. The shear study of Zahn (1987) showed mixed results for saline ice adhesion to Standard Vellox but overall is supportive of our findings. His mean shear value for Vellox was only 5% lower than that for TTE-490; too similar to identify a preference for one over the other due to large scatter in the data. However, only nine Vellox samples built up enough ice to test and compare with 23 TTE samples because his samples were not dammed. This is a dramatic demonstration of the water repellency of Vellox under a specific set of ice growth conditions. The nine Vellox samples that did have enough ice to test had, on average, 10% less surface area covered by ice than the TTE samples. When re-evaluated using "effective" bond strengths (the mean shear values divided by the contact area of the ice), Zahn's data show 20% greater adhesion for Vellox than the Navy standard. These new values still did not allow the statistical resolution of the preferred coating. Since our spray icing arrangement produced 100% ice coverage on all samples, these results should be compared to the effective bond strengths of Zahn. With a high level of certainty (98% confidence level), this study shows a 31% greater bond strength for Standard Vellox over TTE. The other versions of Vellox, GV and BV, had 22% and 66% greater bond strength than TTE.

Our results combined with those of Zahn indicate that Vellox has favorable fresh and saline water-shedding qualities that make it an attractive anti-icing coating. However, based strictly on adhesive shear strength, FPC and the three versions of Vellox are less desirable for de-icing freshwater accretions than is the Navy's standard topcoat, TTE-490.

## CONCLUSIONS

The test used in this study to evaluate adhesion strength was not intended to be a true shear test. Shear loading is ideally accomplished by applying a uniformly distributed load over the entire bulk of the ice. The edge loading approach taken in this study was dictated by the need for simplicity and economy. The objective of our test was to induce adhesion failure at the ice/substrate interface in a controlled and reproducible manner. The resulting failure surfaces indicated that shearing failures were obtained by the edge loading technique used.

Results showed that all four of the experimental coatings exhibited higher mean shear values than the standard Navy deck paint, TTE-490. The mean shear values for the surfaces tested were very similar in absolute magnitude, ranging from 71.6 to 119.2 kPa, with relative percentage deviation in shear values ranging from 15 to 28% of the total stress. A nonparametric statistical analysis showed with greater than 96% confidence that TTE-490 had significantly lower adhesion strength for freshwater spray ice than the four candidate coatings.

It should be noted that under certain meteorological conditions and surface configurations, water may be shed from Vellox-coated surfaces before freezing can occur so that total accretion amounts may be reduced. However, given cold enough conditions, some droplets will freeze and accrete before they can be shed. Once this occurs, these ice particles become sites for additional icing and the rate of accretion approaches that of a non-icephobic surface.

This study shear tested each sample only once. Since a heavy residue of coating was removed along with ice from all the Vellox samples (Standard, Gray, and Black), the question is raised as to its ability to remain effective through repeated icing and deicing cycles. It is therefore suggested that a durability study be conducted on Vellox-140 and its other versions to ascertain its useful lifetime as an anti-icing coating.

## LITERATURE CITED

**Druez, J., D.D. Nguyen and Y. Lavoie** (1986) Mechanical properties of atmospheric ice. *Cold Regions Science and Technology*, **13**: 67–74.

**Free, A.P. and W. Chaney** (1986) Final report on tests of coatings to prevent ship superstructure icing. ARCTEC Engineering, Report 1324C-1.

**Jellinek, H.H.G.** (1960) Adhesive properties of ice: Part II. USA Snow, Ice and Permafrost Research Establishment, Research Report 62.

**Jones, J.R. and M.N. Gardos** (1972) Adhesive shear strength of ice to bonded solid lubricants. *Lubrication Engineering*, **28**(12): 464–471.

**Lyrra, M., M. Jantti and J. Launiainen** (1986) Ad-

hesive strength of spray accreted ice on materials and coatings. In *Proceedings, POLARTECH '86, Helsinki,* vol. 1, p. 484–496.

**Makkonen, L.** (1987) Salinity and growth rate of ice formed by sea spray. *Cold Regions Science and Technology,* **14:** 163–171.

**Norusis, M.J.** (1986) SPSS/PC+ for the IBM PC/XT/AT. SPSS Inc., Chicago.

**Oksanen, P.** (1982) Adhesion strength of ice. Technical Research Center of Finland, Espoo, Research Report 123.

**Richter-Menge, J.A., G.F.N. Cox, N. Perron, G. Durell and H.W. Bosworth** (1986) Triaxial testing of first-year sea ice. USA Cold Regions Research and Engineering Laboratory, CRREL Report 86-16, p. 10.

**Sackinger, W.M.** (1985) Spray ice bonding to superstructure coatings. In *Proceedings, U.S. Navy Symposium on Arctic/Cold Weather Operations of Surface Ships, Washington, D.C., 3–4 Dec 1985,* p. 453–455.

**Savelyev, B.A., V.N. Golubev, M.N. Laptev and I.B. Savelyev** (1972) Structural features of ice adhesion to solids. In *Proceedings, IAHR Symposium on Ice and its Action on Hydraulic Structures, Leningrad,* p. 34–38.

**Sayward, J.M.** (1979) Seeking low ice adhesion. USA Cold Regions Research and Engineering Laboratory, Special Report 79-11.

**Seigel, S.** (1956) *Nonparametric Statistics for the Behavioral Sciences.* New York: McGraw-Hill, p. 116–127 and p. 184–193.

**Shaw, G. and D. Wheeler** (1985) *Statistical Techniques in Geographic Analysis.* New York: John Wiley & Sons, p. 134–142.

**Tashman, L.J. and K.R. Lamborn** (1979) *The Ways and Means of Statistics.* New York: Harcourt Brace Jovanovich, p. 402–410.

**U.S. Navy, Chief of Naval Operations** (1988) U.S. Navy Cold Weather Handbook for Surface Ships. Surface Ship Survivability Office, OPNAV P-03C-01-89.

**Zahn, P.B.** (1987) Coatings to prevent or reduce ship superstructure icing. Phase II laboratory tests. U.S. Maritime Administration, Washington, D.C., U.S. Department of Transportation Report 87-202C-1.

## APPENDIX A: MANUFACTURERS OF CONTROL AND TEST SURFACES.

TTE-490:

Sentry Paint and Chemical Co.
237 Mill Street
Darby, Pennsylvania 19023
(215) 522-1900

Aluminum: (Alca Plus cast-machined plate)

Aluminum Company of America
1501 Alcoa Building
Pittsburgh, Pennsylvania 15219
(412) 553-4545

FPC: (Fluorocarbon Penetrating Coating)

Fluorocarbon Technologies, Inc.
7047-A Bembe Beach Road
Annapolis, Maryland 21403
(301) 268-6451

Vellox-140:

M-Chem Corporation
9 Bishop Road
Ayer, Massachusetts 01432

Sales and Technical Service:
Clifford W. Estes Company
P.O. Box 907
Lindhurst, New Jersey 07071
(201) 935-2550

## APPENDIX B: TEMPERATURE AND ICE THICKNESS MEASUREMENTS DURING ICE GROWTH PERIODS

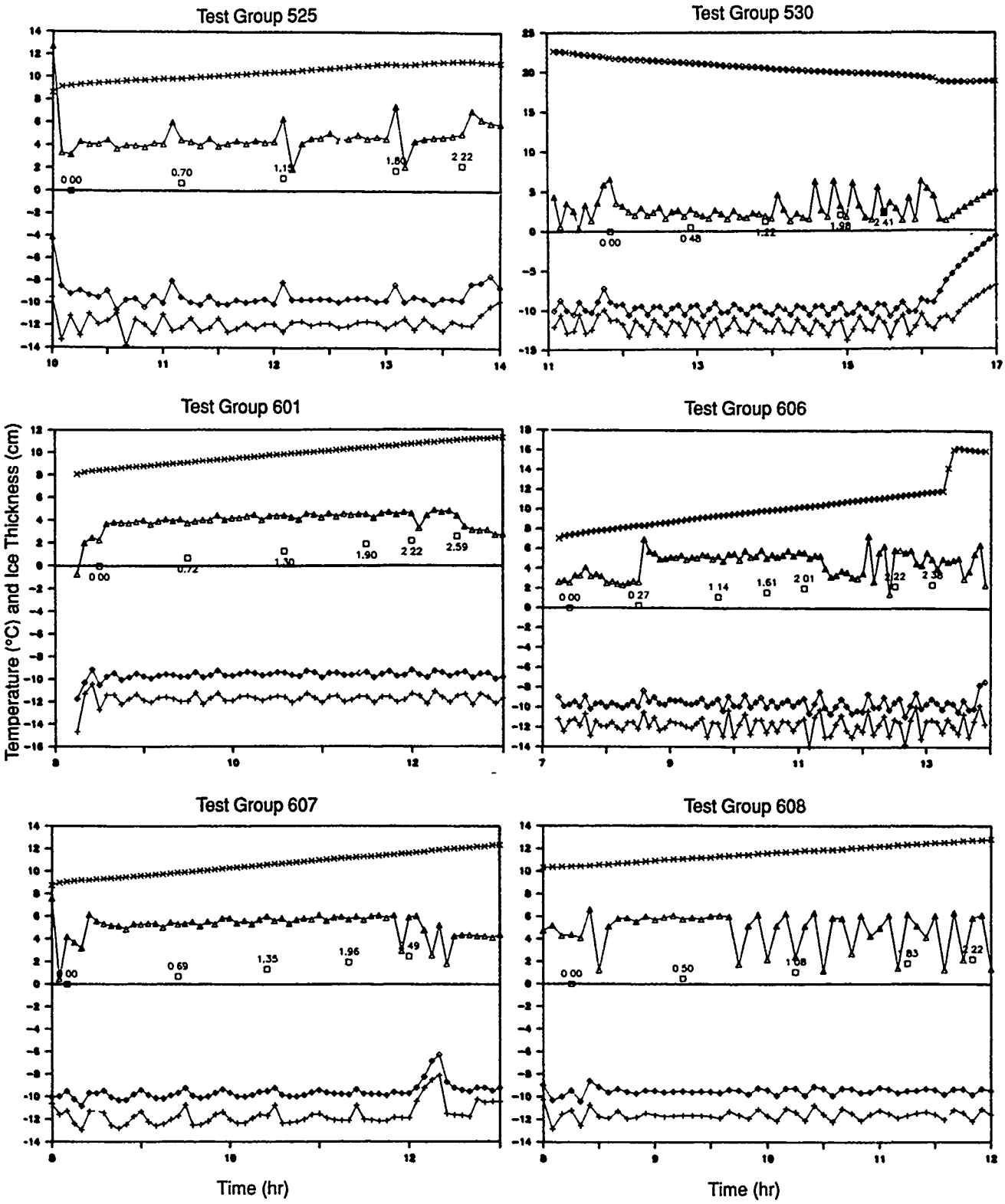

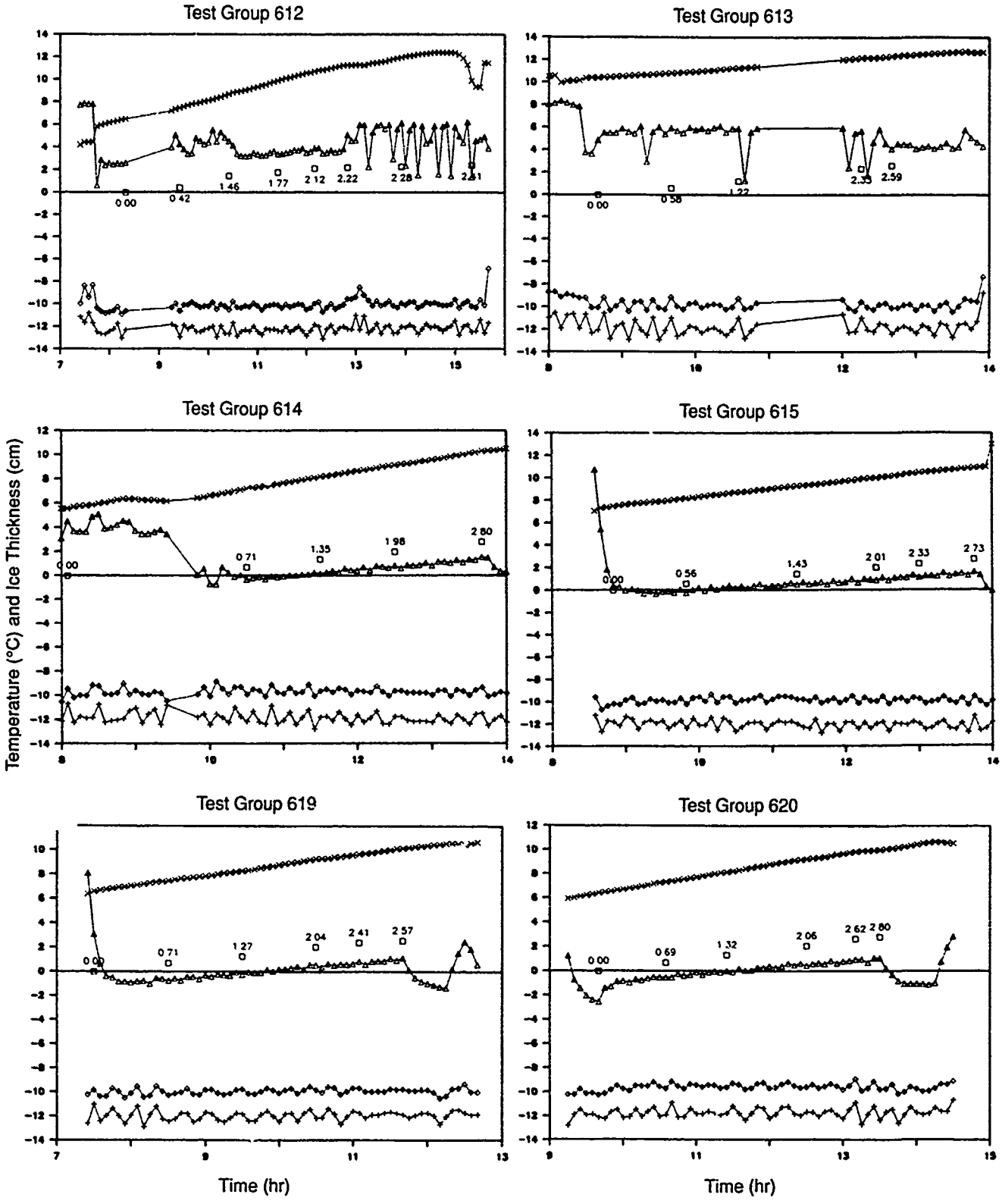
Test Group 612
Test Group 613
Test Group 614
Test Group 615
Test Group 619
Test Group 620
Temperature (°C) and Ice Thickness (cm)
Time (hr)
Time (hr)
Legend: ❑ Ice thickness Δ Nozzle + Room air × Reservoir ◊ Chamber air

APPENDIX C: ADHESION SHEAR TEST LOADING HISTORIES.

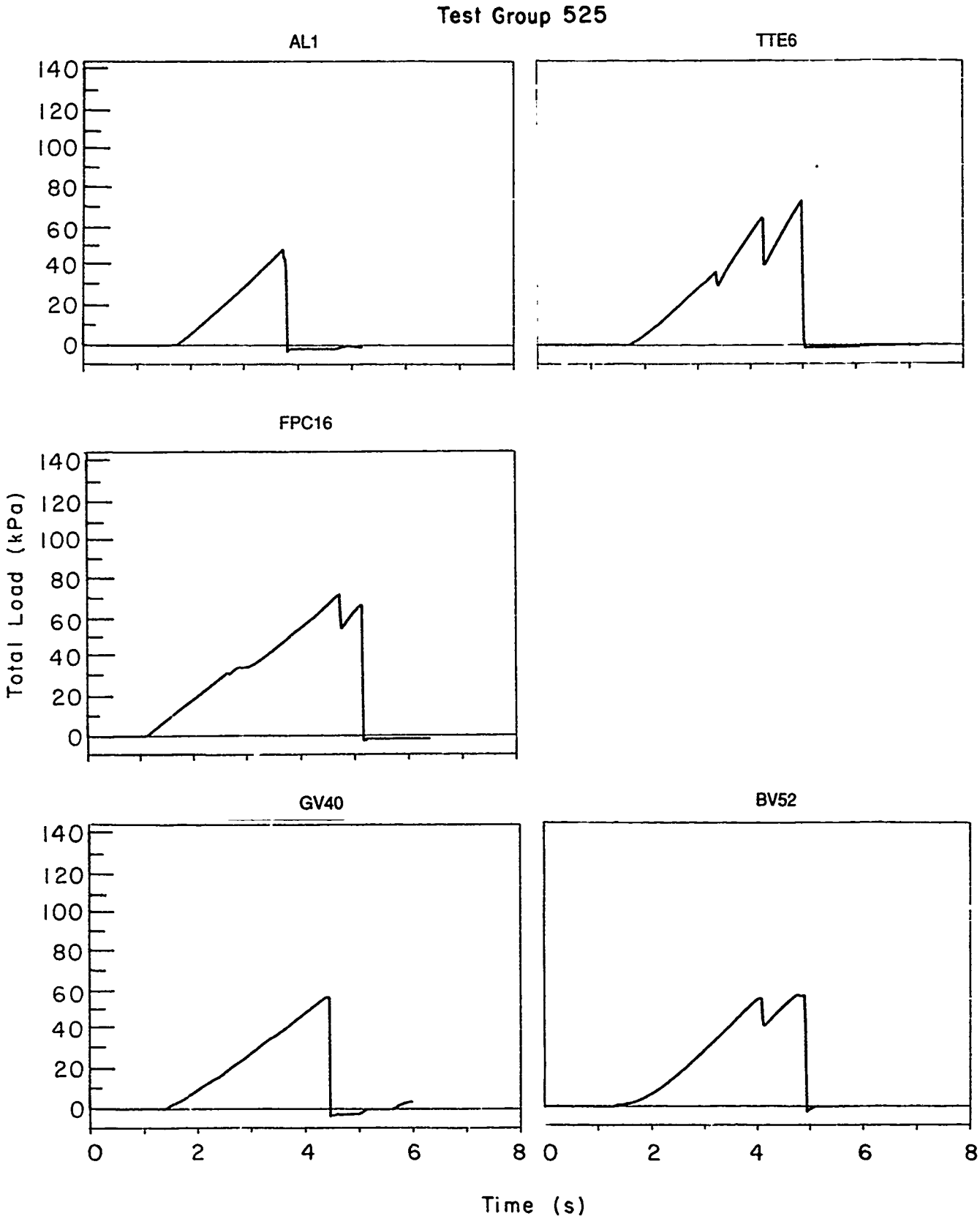

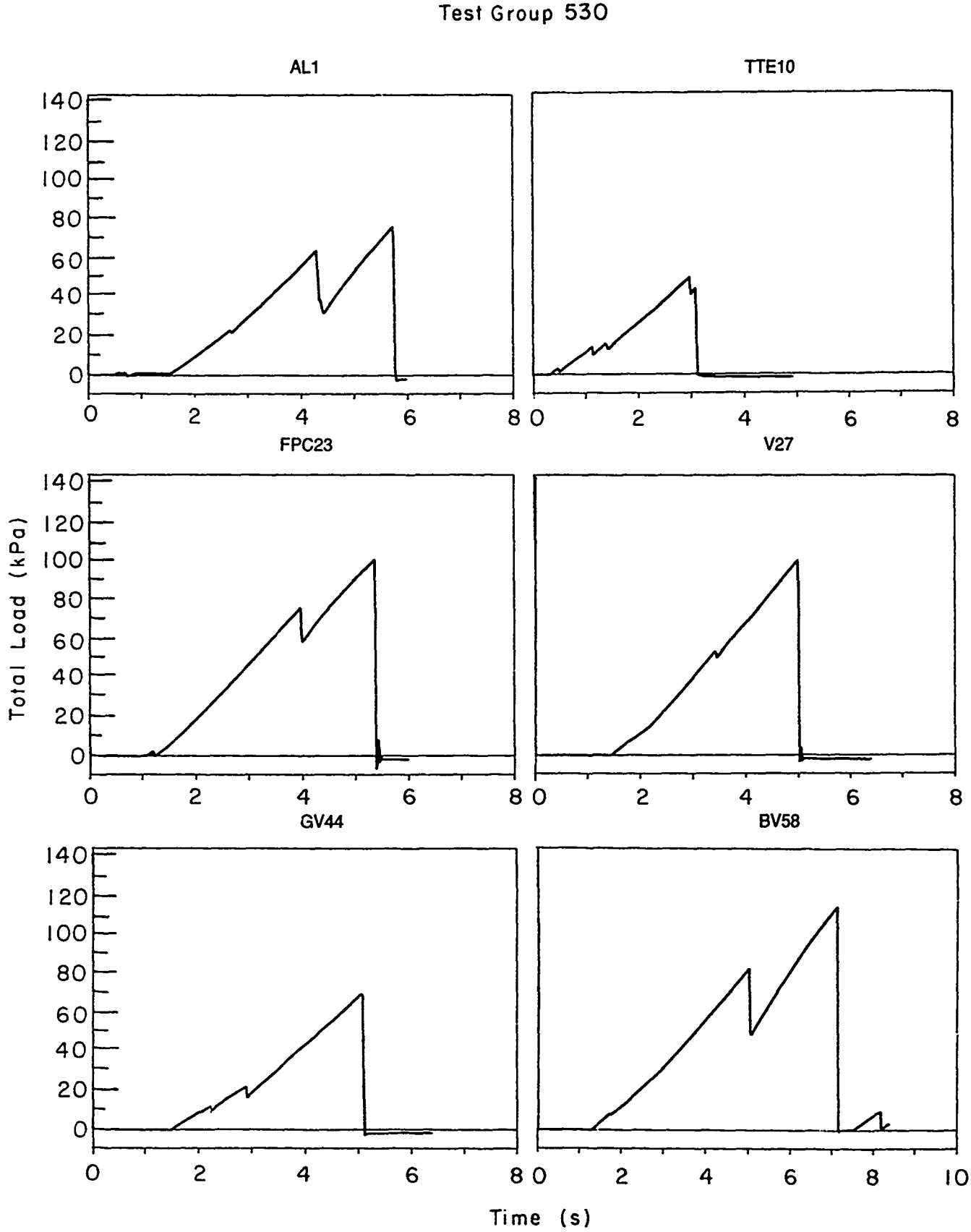
Test Group 530
AL1
TTE10
FPC23
V27
GV44
BV58
Total Load (kPa)
Time (s)
0
20
40
60
80
100
120
140
0
2
4
6
8
10

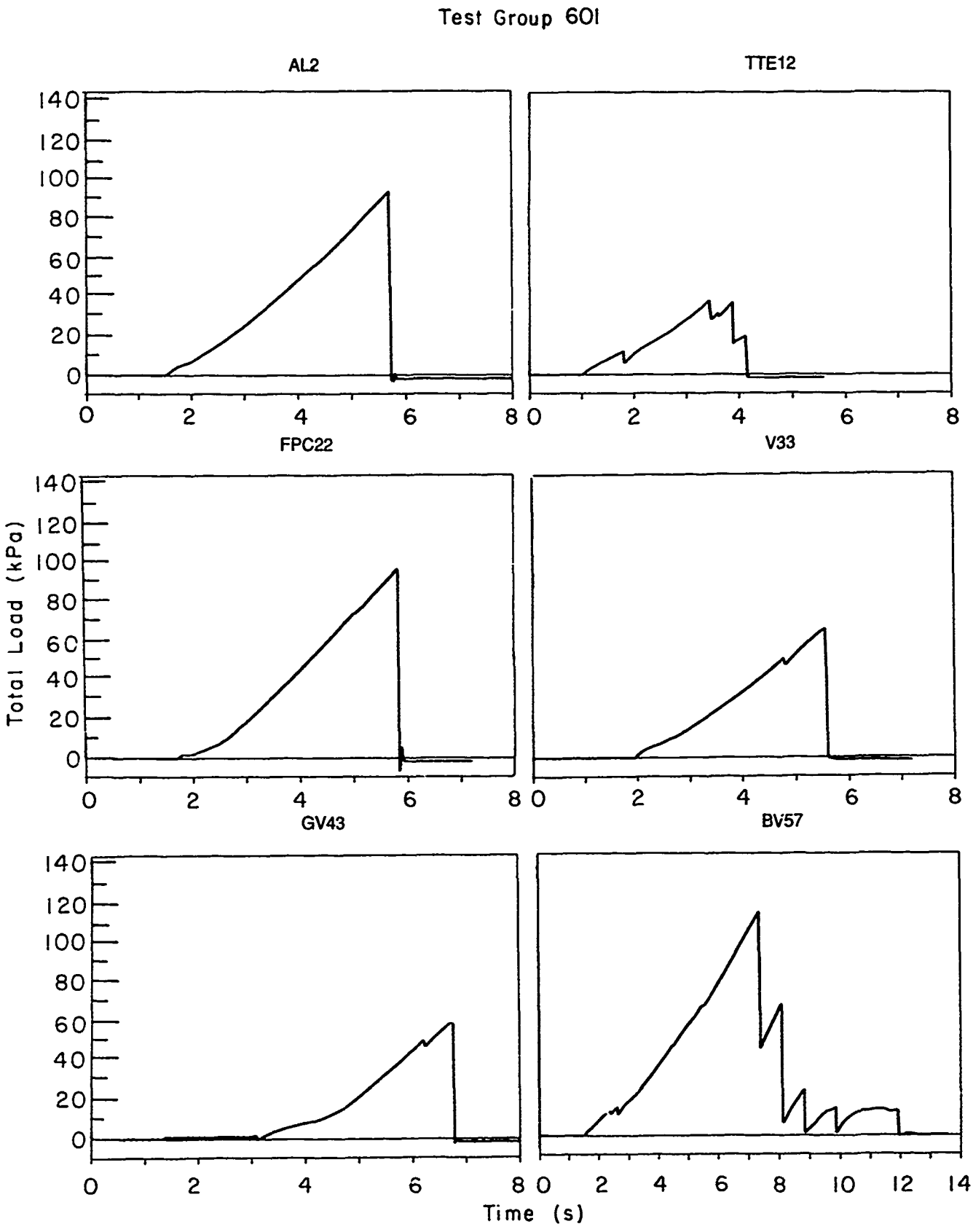
Test Group 601
AL2
TTE12
FPC22
V33
GV43
BV57
Total Load (kPa)
Time (s)
0
20
40
60
80
100
120
140
0
2
4
6
8
10
12
14

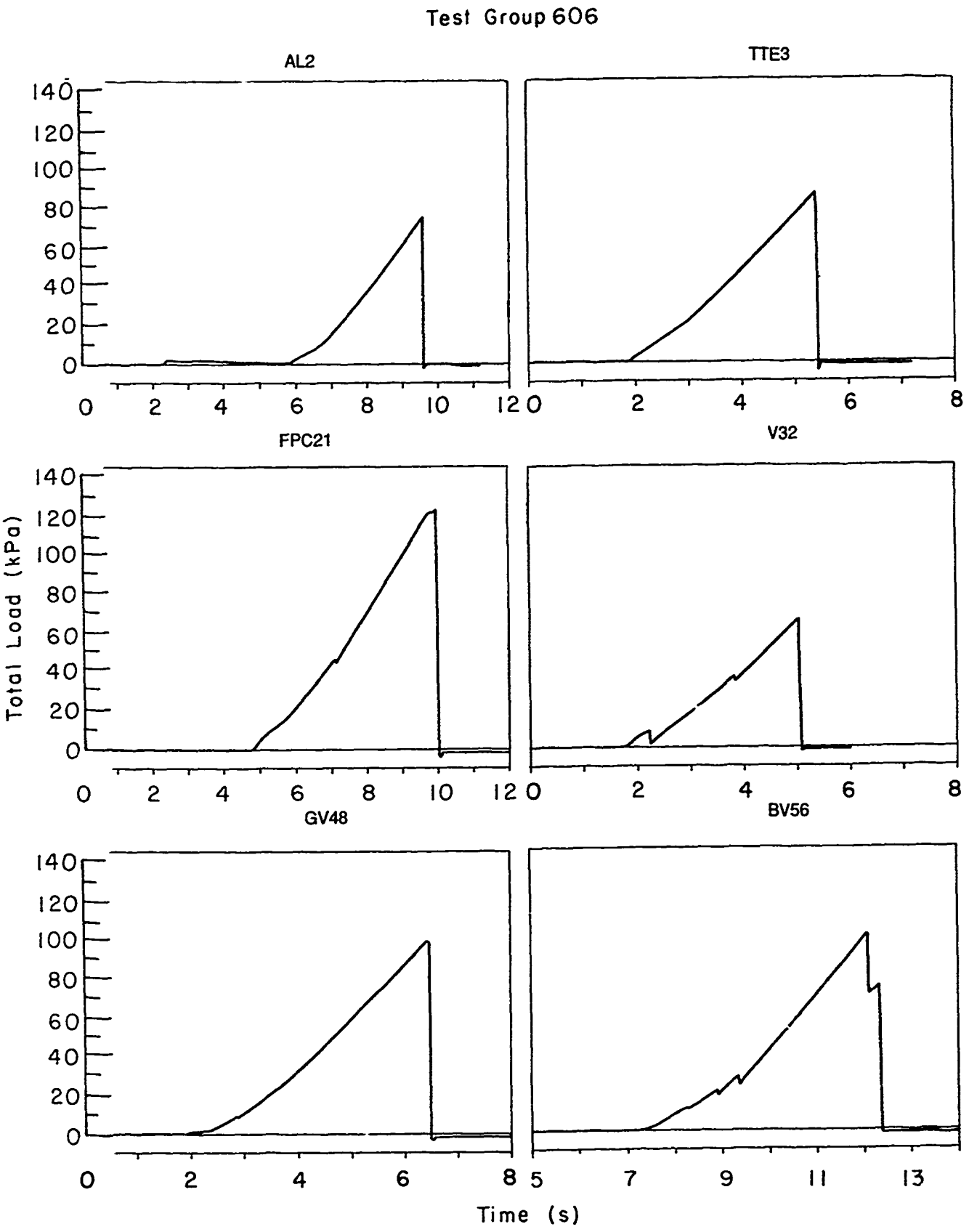
Test Group 606
AL2
TTE3
FPC21
V32
GV48
BV56
Total Load (kPa)
Time (s)
0
20
40
60
80
100
120
140
0
2
4
6
8
10
12
5
7
9
11
13

Test Group 607

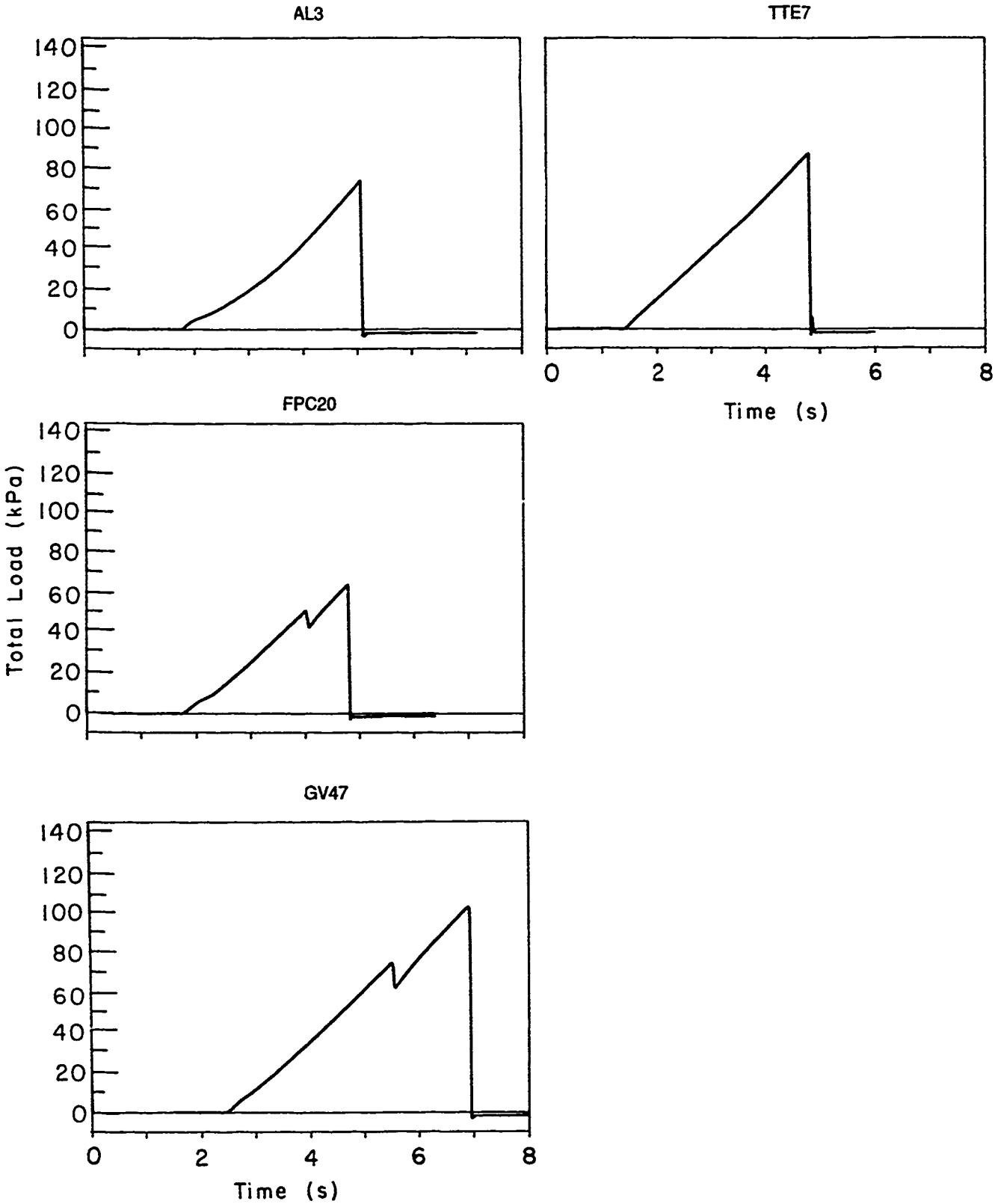

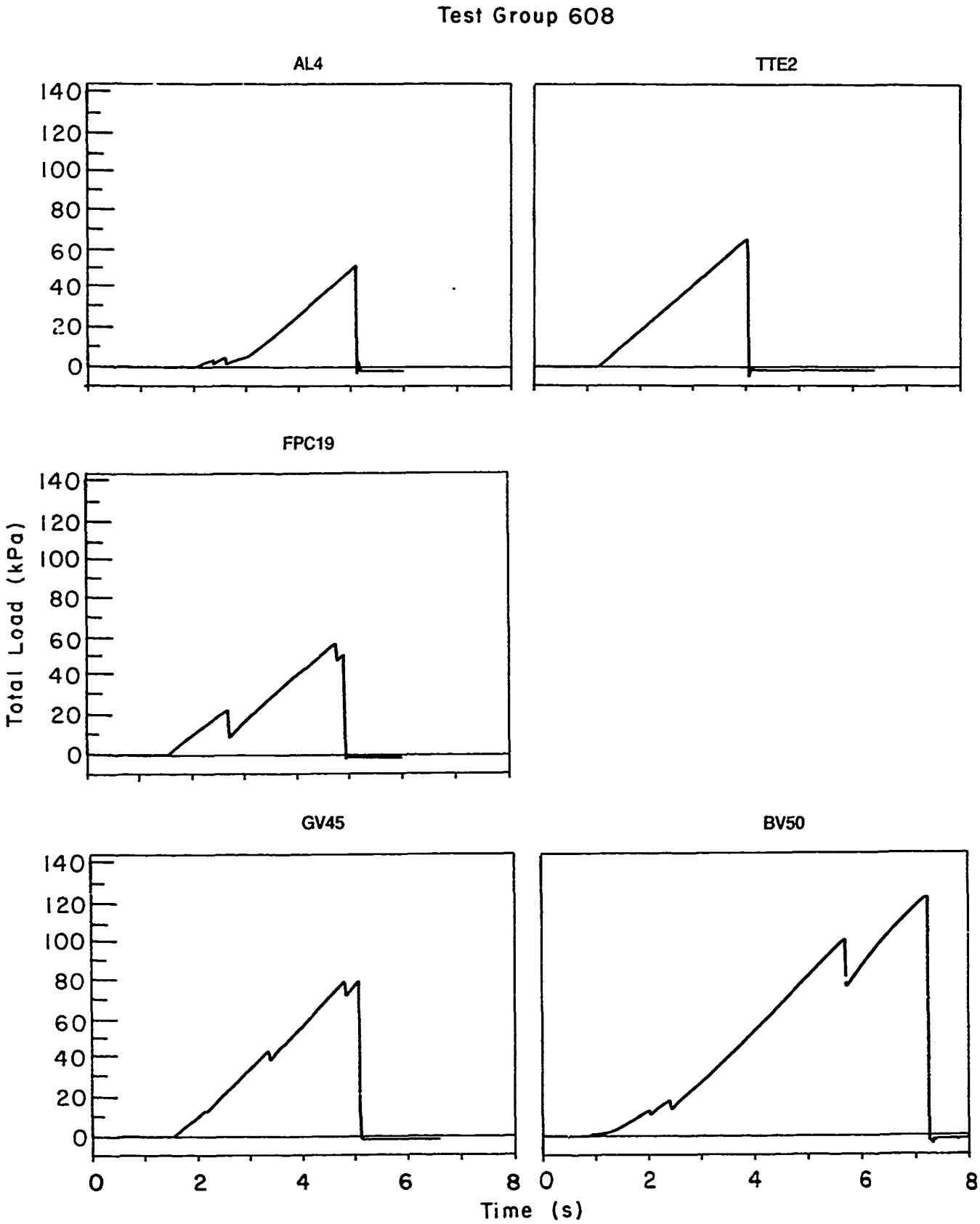
Test Group 608
AL4
TTE2
FPC19
GV45
BV50
Total Load (kPa)
140
120
100
80
60
40
20
0
0
2
4
6
8
Time (s)

Test Group 612

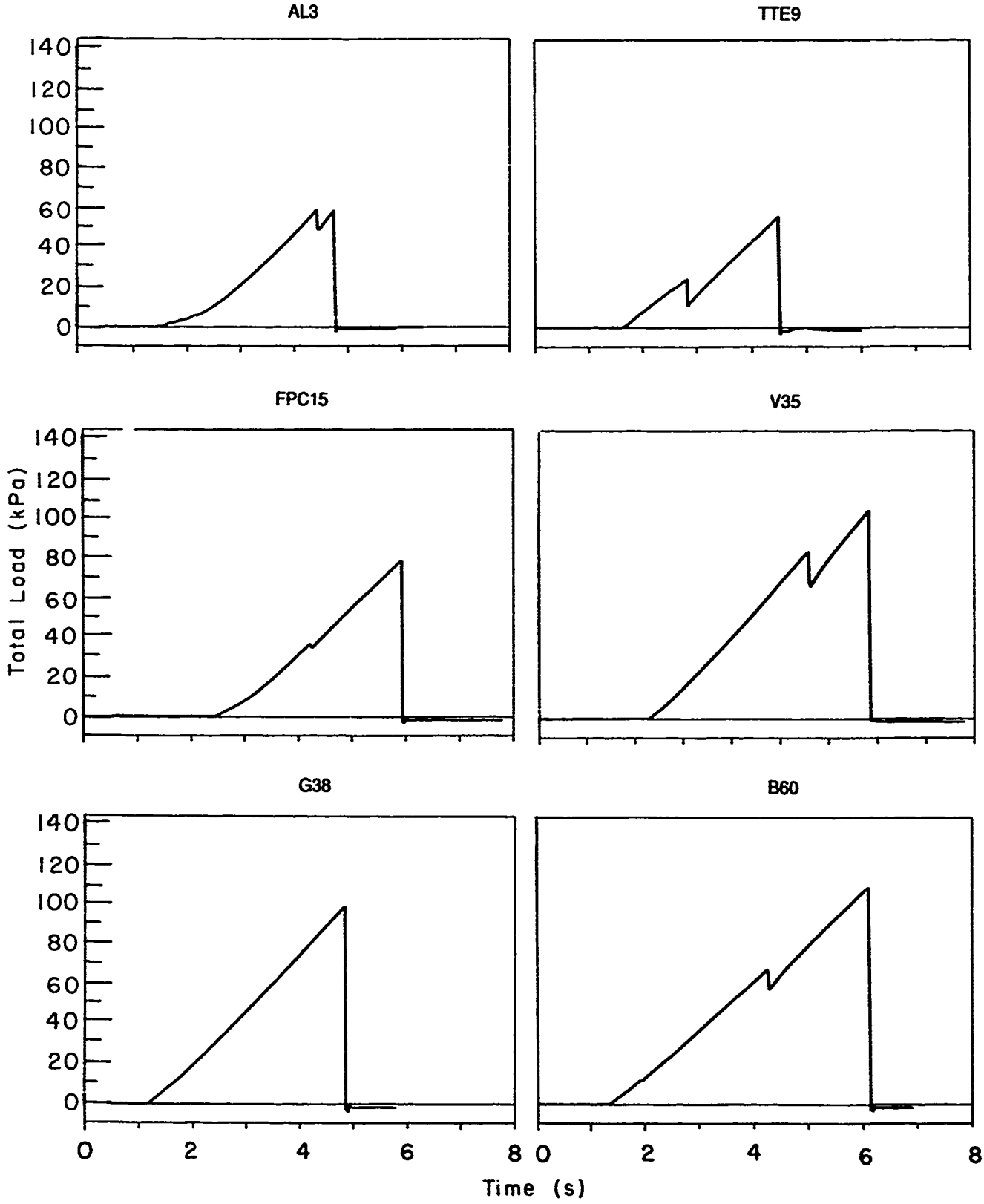

Test Group 613

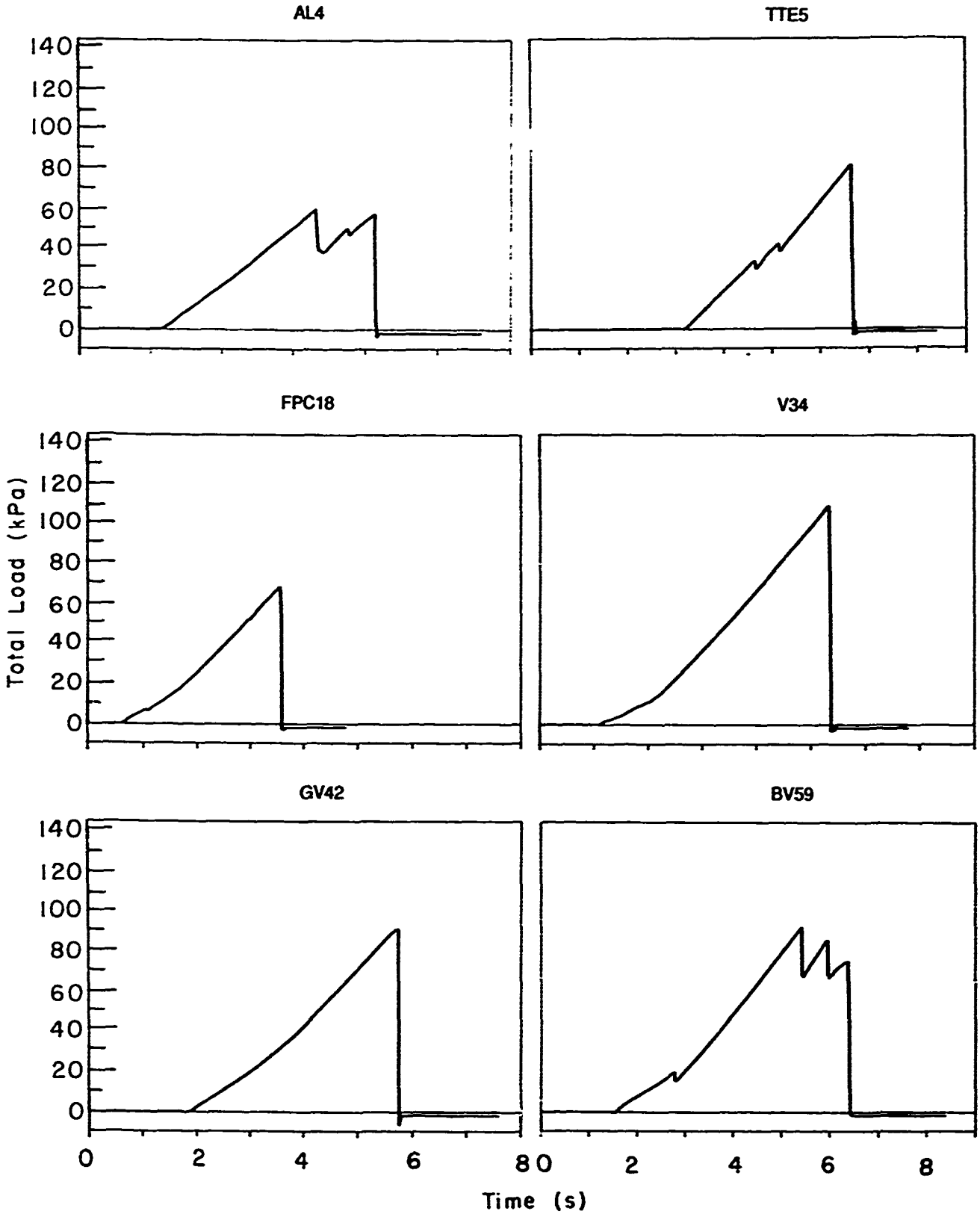

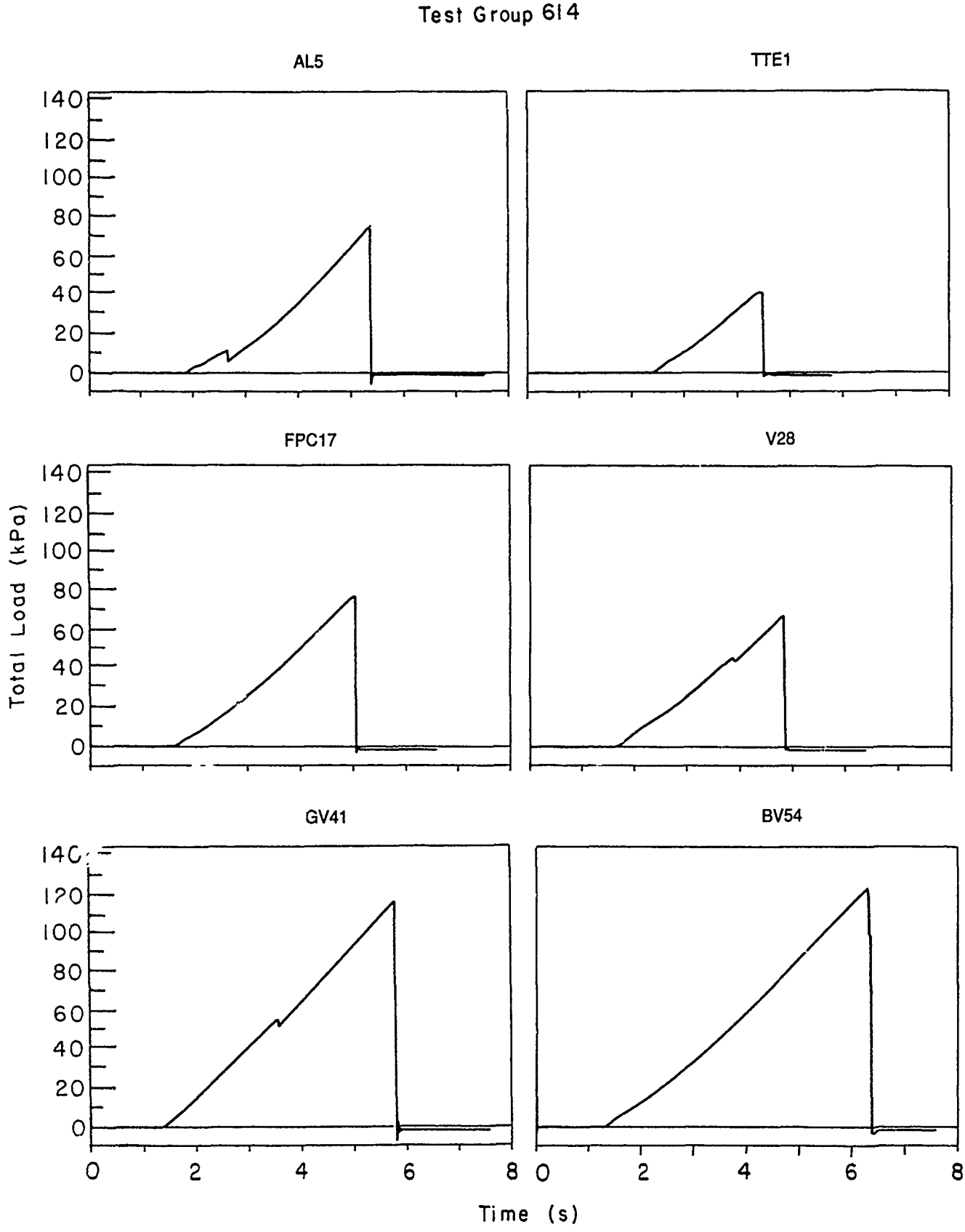
Test Group 614
AL5
TTE1
FPC17
V28
GV41
BV54
Total Load (kPa)
140
120
100
80
60
40
20
0
0
2
4
6
8
Time (s)

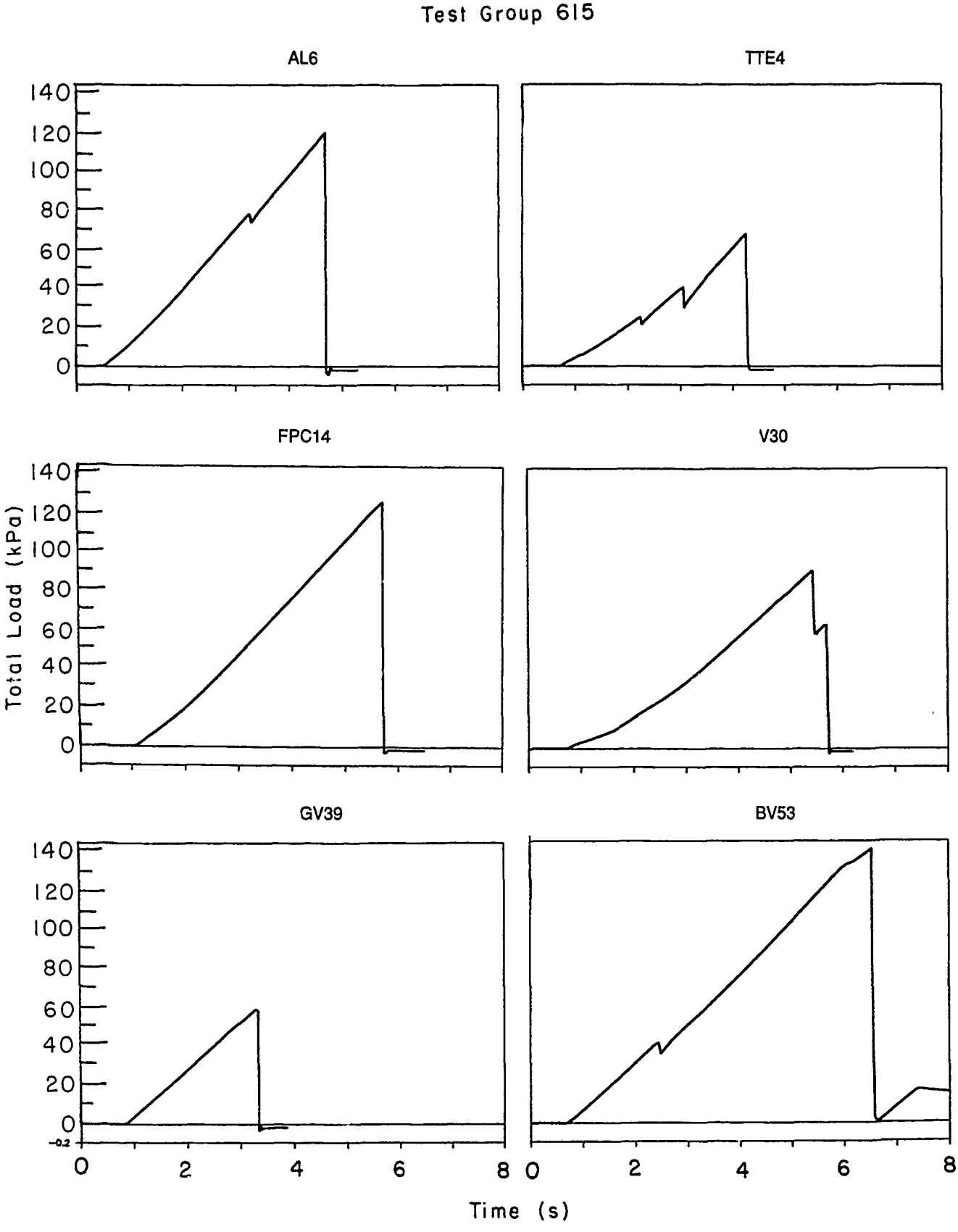
Test Group 615
AL6
TTE4
FPC14
V30
GV39
BV53
Total Load (kPa)
140
120
100
80
60
40
20
0
-0.2
0
2
4
6
8
Time (s)

Test Group 619

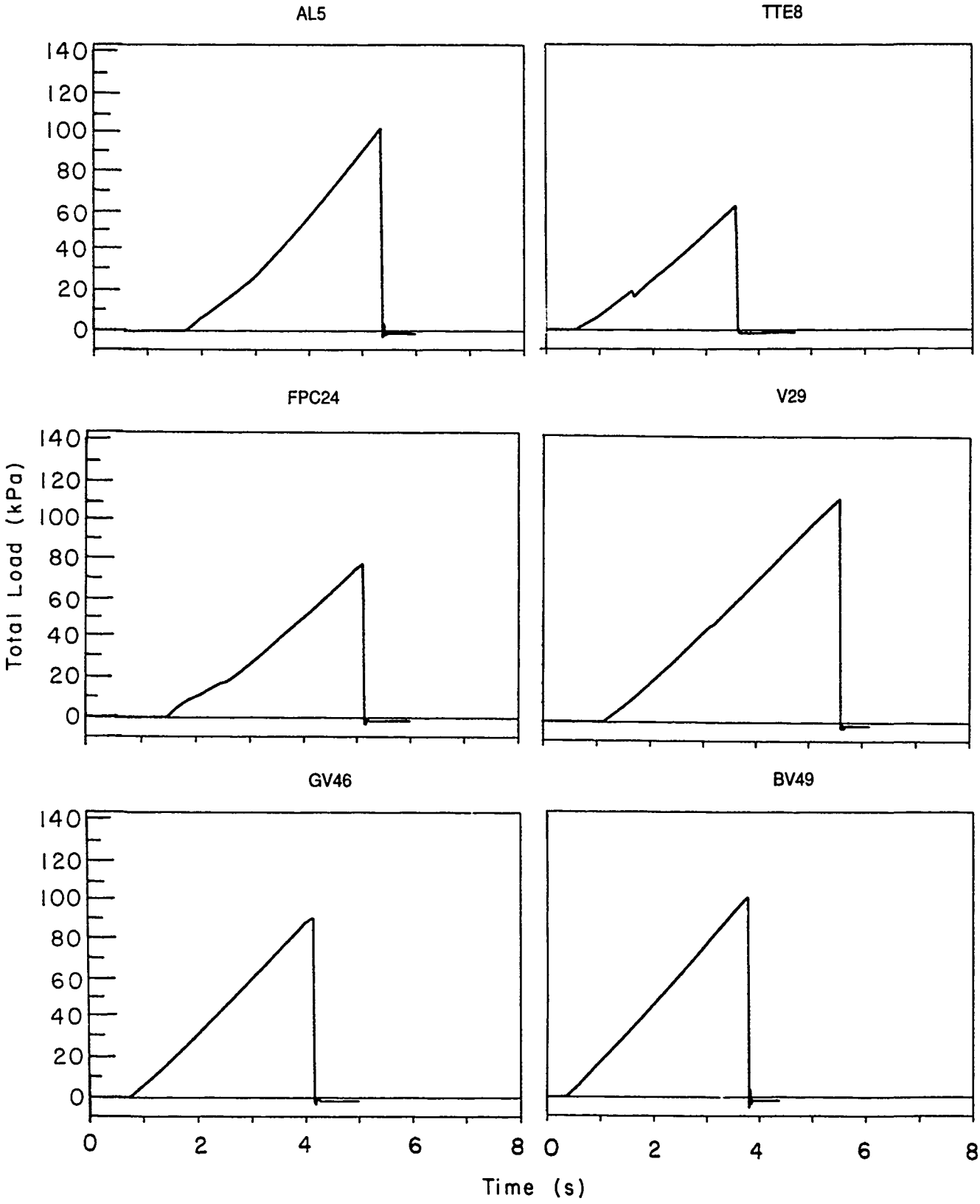

Test Group 620

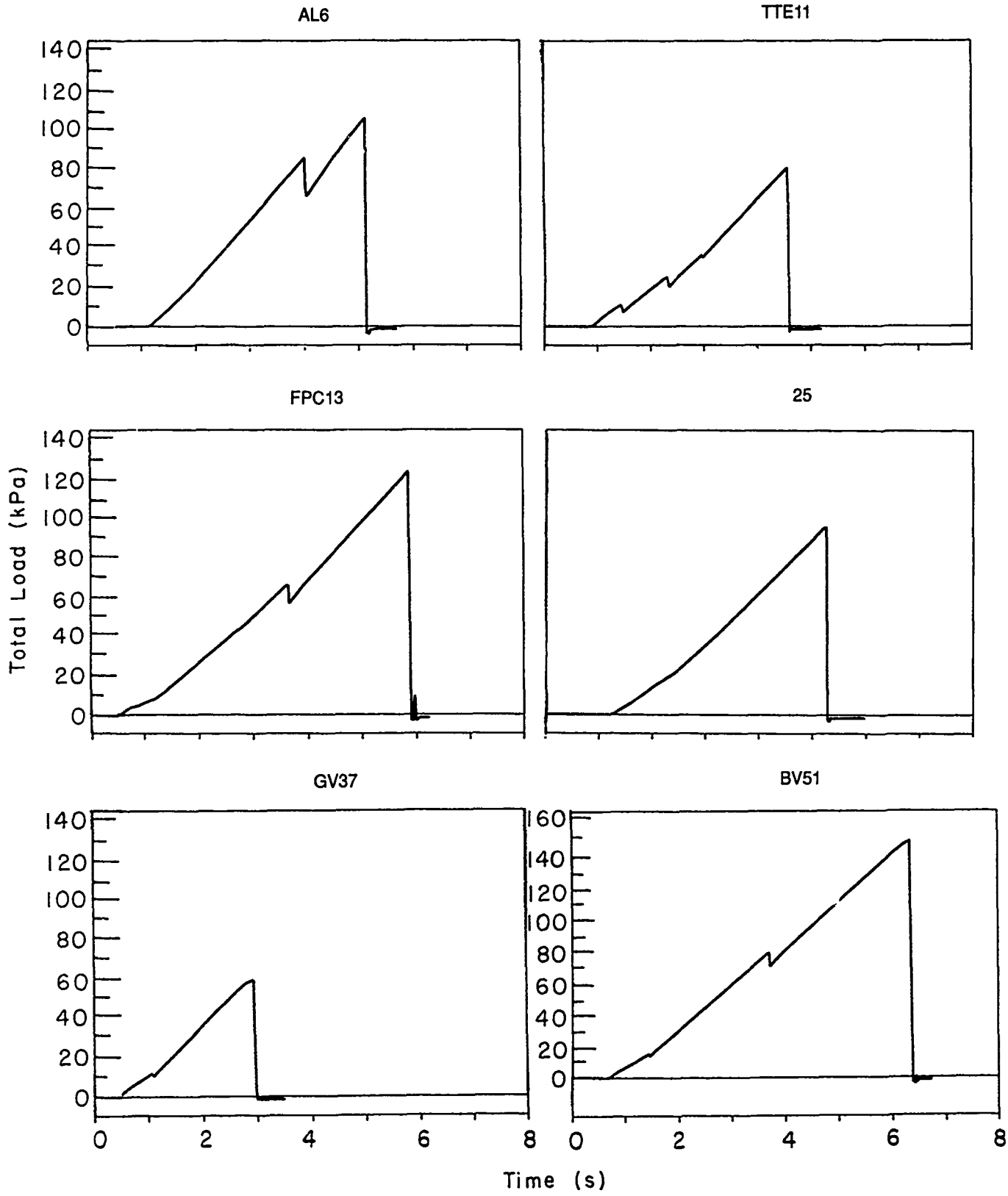

## APPENDIX D: POST-TEST FRACTURE PATTERNS.

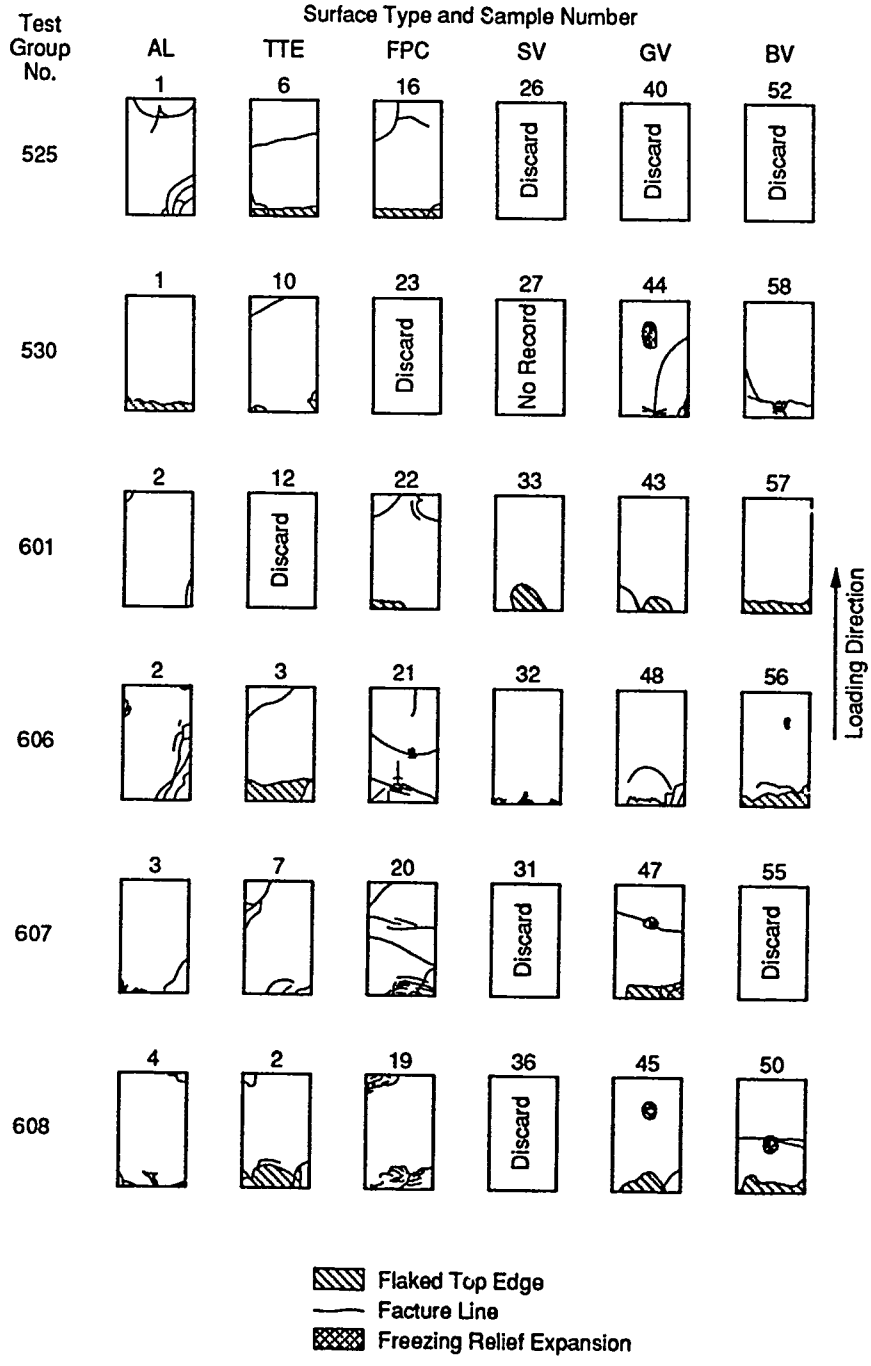

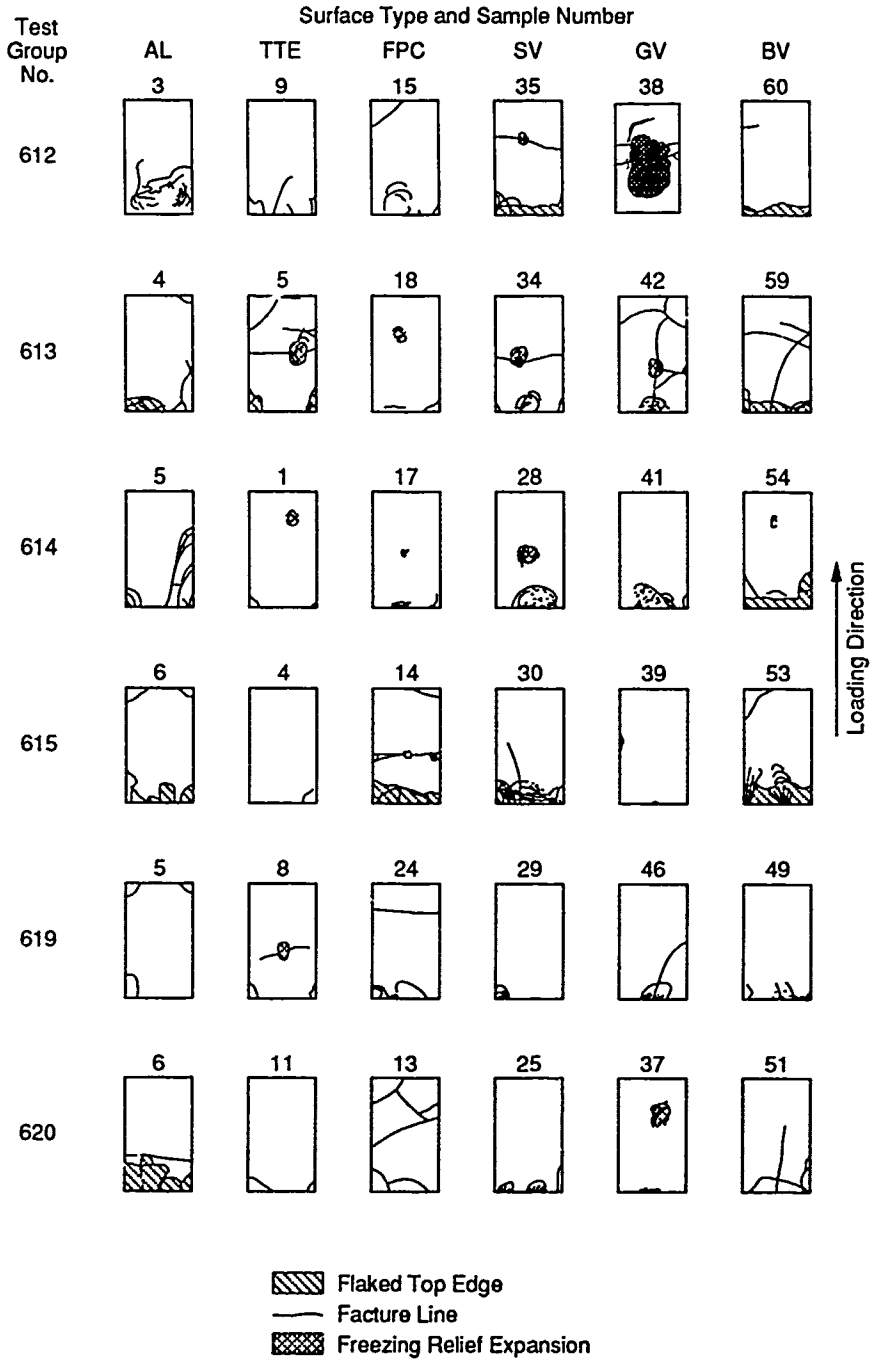
Surface Type and Sample Number
Test Group No.
AL
TTE
FPC
SV
GV
BV
612
3
9
15
35
38
60
613
4
5
18
34
42
59
614
5
1
17
28
41
54
615
6
4
14
30
39
53
619
5
8
24
29
46
49
620
6
11
13
25
37
51
Loading Direction
Flaked Top Edge
Facture Line
Freezing Relief Expansion

## APPENDIX E: THE MANN-WHITNEY TEST FOR STATISTICAL SIGNIFICANCE.

The Mann-Whitney tests on our shear test data were performed in the following manner: The 64 successful tests were ranked in ascending order of peak shear values. Rank scores appear in parentheses with each sample name in Table 2. The value of $U$ is given by the number of times that a score in one group is preceded by the scores of the other group. The following example illustrates the Mann-Whitney test of the scores of TTE-490 samples with those of FPC. The data show that the least-to-greatest adhesion values rank as follows (out of the possible 64 cases):

| | | | | | | | | | | | | |
|---|---|---|---|---|---|---|---|---|---|---|---|---|
| TTE-490 | 1 | 3 | 5 | 12 | 16 | 18 | 22 | 31 | 32 | 33 | 34 | |
| FPC | 6 | 13 | 19 | 21 | 27 | 28 | 29 | 41 | 46 | 60 | 62 | 63 |

The scores are then placed in order:

| | | | | | | | | | | | | | | | | | | | | | | |
|---|---|---|---|---|---|---|---|---|---|---|---|---|---|---|---|---|---|---|---|---|---|---|
| 1 | 3 | 5 | 6 | 12 | 13 | 16 | 18 | 19 | 21 | 22 | 27 | 28 | 29 | 31 | 32 | 33 | 34 | 41 | 46 | 60 | 62 | 63 |
| *T* | *T* | *T* | *F* | *T* | *F* | *T* | *T* | *F* | *F* | *T* | *F* | *F* | *F* | *T* | *T* | *T* | *T* | *F* | *F* | *F* | *F* | *F* |

where $T$ refers to a TTE-490 score and $F$ refers to an FPC score.

We then select the set with the lowest overall values (in this case, TTE-490) as our "object group," and count the number of times a value from the other group precedes each value from the object group. The first three TTE-490 scores have no FPC scores preceding it. The fourth $T$ score is preceded by one $F$ score, the fifth $T$ score is preceded by two $F$ scores, and so on. The test statistic, $U$ is the sum of these counts:

$$U = 0 + 0 + 0 + 1 + 2 + 2 + 4 + 7 + 7 + 7 + 7 = 37$$

When the number of samples in the larger group is between 9 and 20, the confidence test is made by using tables which identify a specific probability value associated with the calculated $U$-value. The tables have been reproduced as Tables E1–E3. The $U$-value must be less than or equal to the critical $U$ for the null hypothesis to be rejected at each table's significance level. In our example, we have 11 samples in the TTE group and 12 in the other ($n_1 = 11$ and $n_2 = 12$). One-tailed probabilities were used since we want to know if one coating is better than another. At the 0.025 (Table E2) and 0.05 (Table E3) significance levels, the critical $U$-values are 33 and 38, respectively. The $U$ statistic of 37 is greater than the critical $U$ of the 0.025 significance level but less than that of the 0.05 level. This means that the probability $p$ of obtaining identical mean shear values by chance variation when the means are actually different, is between 2.5 and 5.0%, based on the test results.

The level of confidence $C$ that we have in the data, usually stated as a percentage is defined as

$$C = (1-p)$$

Therefore, the null hypothesis (TTE and FPC have the same affinity for ice) can be rejected with between 95 and 97.5% confidence in favor of the alternate hypothesis (TTE-490 has a lower affinity for ice than does FPC). The figure shown in Table 3 at the TTE column and the FPC row (0.9604, or 96%) is the computer-generated interpolation of significance.

**Table E1. Critical values of the Mann-Whitney test statistic $U^*$. Significance level = 0.02 (two-tailed) or 0.01 (one-tailed).**

| $n_1$ / $n_2$ | 9 | 10 | 11 | 12 | 13 | 14 | 15 | 16 | 17 | 18 | 19 | 20 |
|---|---|---|---|---|---|---|---|---|---|---|---|---|
| 2 | | | | | 0 | 0 | 0 | 0 | 0 | 0 | 1 | 1 |
| 3 | 1 | 1 | 1 | 2 | 2 | 2 | 3 | 3 | 4 | 4 | 4 | 5 |
| 4 | 3 | 3 | 4 | 5 | 5 | 6 | 7 | 7 | 8 | 9 | 9 | 10 |
| 5 | 5 | 6 | 7 | 8 | 9 | 10 | 11 | 12 | 13 | 14 | 15 | 16 |
| 6 | 7 | 8 | 9 | 11 | 12 | 13 | 15 | 16 | 18 | 19 | 20 | 22 |
| 7 | 9 | 11 | 12 | 14 | 16 | 17 | 19 | 21 | 23 | 24 | 26 | 28 |
| 8 | 11 | 13 | 15 | 17 | 20 | 22 | 24 | 26 | 28 | 30 | 32 | 34 |
| 9 | 14 | 16 | 18 | 21 | 23 | 26 | 28 | 31 | 33 | 36 | 38 | 40 |
| 10 | 16 | 19 | 22 | 24 | 27 | 30 | 33 | 36 | 38 | 41 | 44 | 47 |
| 11 | 18 | 22 | 25 | 28 | 31 | 34 | 37 | 41 | 44 | 47 | 50 | 53 |
| 12 | 21 | 24 | 28 | 31 | 35 | 38 | 42 | 46 | 49 | 53 | 56 | 60 |
| 13 | 23 | 27 | 31 | 35 | 39 | 43 | 47 | 51 | 55 | 59 | 63 | 67 |
| 14 | 26 | 30 | 34 | 38 | 43 | 47 | 51 | 56 | 60 | 65 | 69 | 73 |
| 15 | 28 | 33 | 37 | 42 | 47 | 51 | 56 | 61 | 66 | 70 | 75 | 80 |
| 16 | 31 | 36 | 41 | 46 | 51 | 56 | 61 | 66 | 71 | 76 | 82 | 87 |
| 17 | 33 | 38 | 44 | 49 | 55 | 60 | 66 | 71 | 77 | 83 | 88 | 93 |
| 18 | 36 | 41 | 47 | 53 | 59 | 65 | 70 | 76 | 82 | 86 | 94 | 100 |
| 19 | 38 | 44 | 50 | 56 | 63 | 69 | 75 | 82 | 88 | 94 | 101 | 107 |
| 20 | 40 | 47 | 53 | 60 | 67 | 73 | 80 | 87 | 93 | 100 | 107 | 114 |

The null hypothesis is rejected if the test statistic ($U$) is less than or equal to the critical value for the larger and smaller group sizes ($n_1$ and $n_2$, respectively) at the selected significance level.

* From Shaw and Wheeler (1985).

**Table E2. Critical values of the Mann-Whitney test statistic *U**. Significance level = 0.05 (two-tailed) or 0.025 (one-tailed).**

| $n_2$ \ $n_1$ | 9 | 10 | 11 | 12 | 13 | 14 | 15 | 16 | 17 | 18 | 19 | 20 |
|---|---|---|---|---|---|---|---|---|---|---|---|---|
| 2 | 0 | 0 | 0 | 1 | 1 | 1 | 1 | 1 | 2 | 2 | 2 | 2 |
| 3 | 2 | 3 | 3 | 4 | 4 | 5 | 5 | 6 | 6 | 7 | 7 | 8 |
| 4 | 4 | 5 | 6 | 7 | 8 | 9 | 10 | 11 | 11 | 12 | 13 | 13 |
| 5 | 7 | 8 | 9 | 11 | 12 | 13 | 14 | 15 | 17 | 18 | 19 | 20 |
| 6 | 10 | 11 | 13 | 14 | 16 | 17 | 19 | 21 | 22 | 24 | 25 | 27 |
| 7 | 12 | 14 | 16 | 18 | 20 | 22 | 24 | 26 | 28 | 30 | 32 | 34 |
| 8 | 15 | 17 | 19 | 22 | 24 | 26 | 29 | 31 | 34 | 36 | 38 | 41 |
| 9 | 17 | 20 | 23 | 26 | 28 | 31 | 34 | 37 | 39 | 42 | 45 | 48 |
| 10 | 20 | 23 | 26 | 29 | 33 | 36 | 39 | 42 | 45 | 48 | 52 | 55 |
| 11 | 23 | 26 | 30 | 33 | 37 | 40 | 44 | 47 | 51 | 55 | 58 | 62 |
| 12 | 26 | 29 | 33 | 37 | 41 | 45 | 49 | 53 | 57 | 61 | 65 | 69 |
| 13 | 28 | 33 | 37 | 41 | 45 | 50 | 54 | 59 | 63 | 67 | 72 | 76 |
| 14 | 31 | 36 | 40 | 45 | 50 | 55 | 59 | 64 | 67 | 74 | 78 | 83 |
| 15 | 34 | 39 | 44 | 49 | 54 | 59 | 64 | 70 | 75 | 80 | 85 | 90 |
| 16 | 37 | 42 | 47 | 53 | 59 | 64 | 70 | 75 | 81 | 86 | 92 | 98 |
| 17 | 39 | 45 | 51 | 57 | 63 | 67 | 75 | 81 | 87 | 93 | 99 | 105 |
| 18 | 42 | 48 | 55 | 61 | 67 | 74 | 80 | 86 | 93 | 99 | 106 | 112 |
| 19 | 45 | 52 | 58 | 65 | 72 | 78 | 85 | 92 | 99 | 106 | 113 | 119 |
| 20 | 48 | 55 | 62 | 69 | 76 | 83 | 90 | 98 | 105 | 112 | 119 | 127 |

The null hypothesis is rejected if the test statistic ($U$) is less than or equal to the critical value for the larger and smaller group sizes ($n_1$ and $n_2$, respectively) at the selected significance level.

*From Shaw and Wheeler (1985).

**Table E3. Critical values of the Mann-Whitney test statistic *U**. Significance level = 0.10 (two-tailed) or 0.05 (one-tailed).**

| $n_1$ / $n_2$ | 9 | 10 | 11 | 12 | 13 | 14 | 15 | 16 | 17 | 18 | 19 | 20 |
|---|---|---|---|---|---|---|---|---|---|---|---|---|
| 1 | | | | | | | | | | | 0 | 0 |
| 2 | 1 | 1 | 1 | 2 | 2 | 2 | 3 | 3 | 4 | 4 | 4 | 4 |
| 3 | 3 | 4 | 5 | 5 | 6 | 7 | 7 | 8 | 9 | 9 | 10 | 11 |
| 4 | 6 | 7 | 8 | 9 | 10 | 11 | 12 | 14 | 15 | 16 | 17 | 18 |
| 5 | 9 | 11 | 12 | 13 | 15 | 16 | 18 | 19 | 20 | 22 | 23 | 25 |
| 6 | 12 | 14 | 16 | 17 | 19 | 21 | 23 | 25 | 26 | 28 | 30 | 32 |
| 7 | 15 | 17 | 19 | 21 | 24 | 26 | 28 | 30 | 33 | 35 | 37 | 39 |
| 8 | 18 | 20 | 23 | 26 | 28 | 31 | 33 | 36 | 39 | 41 | 44 | 47 |
| 9 | 21 | 24 | 27 | 30 | 33 | 36 | 39 | 42 | 45 | 48 | 51 | 54 |
| 10 | 24 | 27 | 31 | 34 | 37 | 41 | 44 | 48 | 51 | 55 | 58 | 62 |
| 11 | 27 | 31 | 34 | 38 | 42 | 46 | 50 | 54 | 57 | 61 | 65 | 69 |
| 12 | 30 | 34 | 38 | 42 | 47 | 51 | 55 | 60 | 64 | 68 | 72 | 77 |
| 13 | 33 | 37 | 42 | 47 | 51 | 56 | 61 | 65 | 70 | 75 | 80 | 84 |
| 14 | 36 | 41 | 46 | 51 | 56 | 61 | 66 | 71 | 77 | 82 | 87 | 92 |
| 15 | 39 | 44 | 50 | 55 | 61 | 66 | 72 | 77 | 83 | 88 | 94 | 100 |
| 16 | 42 | 48 | 54 | 60 | 65 | 71 | 77 | 83 | 89 | 95 | 101 | 107 |
| 17 | 45 | 51 | 57 | 64 | 70 | 77 | 83 | 89 | 96 | 102 | 109 | 115 |
| 18 | 48 | 55 | 61 | 68 | 75 | 82 | 88 | 95 | 102 | 109 | 116 | 123 |
| 19 | 51 | 58 | 65 | 72 | 80 | 87 | 94 | 101 | 109 | 116 | 123 | 130 |
| 20 | 54 | 62 | 69 | 77 | 84 | 92 | 100 | 107 | 115 | 123 | 130 | 138 |

The null hypothesis is rejected if the test statistic ($U$) is less than or equal to the critical value for the larger and smaller group sizes ($n_1$ and $n_2$, respectively) at the selected significance level.

* From Shaw and Wheeler (1985).

# REPORT DOCUMENTATION PAGE

*Form Approved*
*OMB No. 0704-0188*



| 1. AGENCY USE ONLY (Leave blank) | 2. REPORT DATE | 3. REPORT TYPE AND DATES COVERED |
|---|---|---|
| | May 1990 | |

**4. TITLE AND SUBTITLE**

Laboratory Test for Measurement of Adhesion Strength of Spray Ice to Coated Flat Plates

**5. FUNDING NUMBERS**

MIPR N0002489MP*

**6. AUTHORS**

Nathan D. Mulherin, Jacqueline A. Richter-Menge, Thomas J. Tantillo, Larry D. Gould, Glenn D. Durell, and Bruce C. Elder

**7. PERFORMING ORGANIZATION NAME(S) AND ADDRESS(ES)**

U.S. Army Cold Regions Research and Engineering Laboratory
72 Lyme Road
Hanover, New Hampshire 03755-1290

**8. PERFORMING ORGANIZATION REPORT NUMBER**

CRREL Report 90-2

**9. SPONSORING/MONITORING AGENCY NAME(S) AND ADDRESS(ES)**

Naval Sea Systems Command
U.S. Department of the Navy
Washington, D.C. 20362

**10. SPONSORING/MONITORING AGENCY REPORT NUMBER**

**11. SUPPLEMENTARY NOTES**

*Additional funding provided by DA Project 4A762730AT42, Task SS, Work Unit 005

**12a. DISTRIBUTION/AVAILABILITY STATEMENT**

Approved for public release; distribution is unlimited.

**12b. DISTRIBUTION CODE**

**13. ABSTRACT** (*Maximum 200 words*)

Four commercial icephobic coatings were selected as candidates for preventing and/or easing the removal of seaspray and atmospheric icing on shipboard superstructures. This study was undertaken to compare the force required to shear freshwater ice from flat test plates coated with the candidate materials. Twelve replicates each of the four different coatings and two different control surfaces (a total of 72 samples) were subjected to laboratory spray icing. The samples were iced and shear tested at −10 ± 1°C at a constant crosshead displacement rate of 0.0381 cm/s. This shear rate was higher by at least an order of magnitude than that in most previous shear studies, ensuring a brittle failure at the ice/coating interface. The method produced virtually 100% ice/coating abhesion in every test, which eliminated analysis problems associated with cohesive failure. Results showed that all four of the experimental coatings exhibited higher mean shear values than either of the two controls. Although the mean shear values for the various coatings were very similar in absolute magnitude, ranging from 71 to 119 kPa, statistical analysis showed a significant difference in surface performance with greater than 97% confidence.

**14. SUBJECT TERMS**

Adhesion shear strength
Freshwater ice
Ice-resistant coatings
Ice removal
Ship icing

**15. NUMBER OF PAGES**

52

**16. PRICE CODE**

| 17. SECURITY CLASSIFICATION OF REPORT | 18. SECURITY CLASSIFICATION OF THIS PAGE | 19. SECURITY CLASSIFICATION OF ABSTRACT | 20. LIMITATION OF ABSTRACT |
|---|---|---|---|
| UNCLASSIFIED | UNCLASSIFIED | UNCLASSIFIED | UL |